# Accepted Manuscript

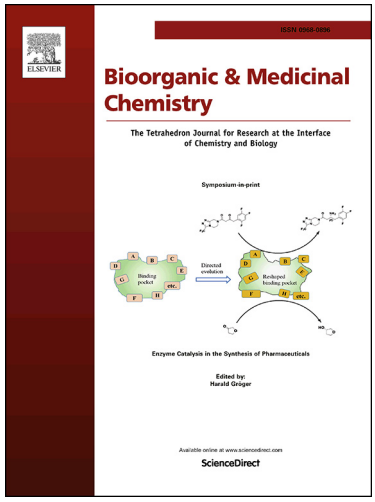


Rational modification of Mannich base-type derivatives as novel antichagasic compounds: synthesis, *in vitro* and *in vivo* evaluation

Rocío Paucar, Rubén Martín-Escolano, Elsa Moreno-Viguri, Amaya Azqueta, Nuria Cirauqui, Clotilde Marín, Manuel Sánchez-Moreno, Silvia Pérez-Silanes

PII: S0968-0896(19)30711-4
DOI: https://doi.org/10.1016/j.bmc.2019.07.029
Reference: BMC 15013

To appear in: *Bioorganic & Medicinal Chemistry*

Received Date: 2 May 2019
Revised Date: 10 July 2019
Accepted Date: 17 July 2019

Please cite this article as: Paucar, R., Martín-Escolano, R., Moreno-Viguri, E., Azqueta, A., Cirauqui, N., Marín, C., Sánchez-Moreno, M., Pérez-Silanes, S., Rational modification of Mannich base-type derivatives as novel antichagasic compounds: synthesis, *in vitro* and *in vivo* evaluation, *Bioorganic & Medicinal Chemistry* (2019), doi: https://doi.org/10.1016/j.bmc.2019.07.029

This is a PDF file of an unedited manuscript that has been accepted for publication. As a service to our customers we are providing this early version of the manuscript. The manuscript will undergo copyediting, typesetting, and review of the resulting proof before it is published in its final form. Please note that during the production process errors may be discovered which could affect the content, and all legal disclaimers that apply to the journal pertain.

ACCEPTED MANUSCRIPT

# Rational modification of Mannich base-type derivatives as novel antichagasic compounds: synthesis, *in vitro* and *in vivo* evaluation

Rocío Paucar[a], Rubén Martín-Escolano[b], Elsa Moreno-Viguri[a], Amaya Azqueta[c], Nuria Cirauqui[d], Clotilde Marín[b], Manuel Sánchez-Moreno[b], Silvia Pérez-Silanes[a*]

[a] *Universidad de Navarra, Department of Pharmaceutical Technology and Chemistry, Instituto de Salud Tropical, Pamplona 31008, Spain.*

[b] *Department of Parasitology. Instituto de Investigación Biosanitaria (ibs.GRANADA), Hospitales Universitarios De Granada/University of Granada, Granada 18071, Spain.*

[c] *Universidad de Navarra, Department of Pharmacology and Toxicology, Pamplona 31008, Spain.*

[d] *Department of Pharmaceutical Sciences, Federal University of Rio de Janeiro, Rio de Janeiro 21949-900, Brazil.*

*****Corresponding author

Dr. Silvia Pérez-Silanes, E-mail: sperez@unav.es. Universidad de Navarra, Department of Pharmaceutical Technology and Chemistry, Faculty of Pharmacy, 31008, Pamplona, Spain.

**Abstract**

The current chemotherapy against Chagas disease is inadequate and insufficient. A series of ten Mannich base-type derivatives have been synthesized to evaluate their *in vitro* antichagasic activity. After a preliminary screening, compounds **7** and **9** were subjected to *in vivo* assays in a murine model. Both compounds caused a substantial decrease in parasitemia in the chronic phase, which was an even better result than that of the reference drug benznidazole. In addition, compound **9** also showed better antichagasic activity during the acute phase. Moreover, metabolite excretion, effect on mitochondrial membrane potential and the inhibition of superoxide dismutase (SOD) studies were also performed to identify their possible mechanism of action. Finally, docking studies proposed a binding mode of the Fe-SOD enzyme similar to our previous series, which validated our design strategy. Therefore, the results suggest that these compounds should be considered for further preclinical evaluation as antichagasic agents.

**Keywords:** Chagas disease, Mannich bases, Superoxide dismutase, *Trypanosoma cruzi*.

ACCEPTED MANUSCRIPT

## 1. Introduction

Chagas disease is a neglected and potentially lethal tropical parasitic disease that continues to be a serious public health problem worldwide.[1] According to the WHO, approximately 6 to 7 million people are infected worldwide and causing more than 7500 deaths annually[2-3]; 70 million people are at risk of infection,[1] and there is an estimated global cost of US$ 7-9 billion per year.[2, 4] *Trypanosoma cruzi* (*T. cruzi*) is the causative agent of this chronic parasitic illness, and its infection could develop into irreversible cardiac or digestive system damage or both in up to 30% of cases.[5-7] Although different strategies have been performed to combat and eradicate this disease in the last 25 years, there are still some gaps that need to be resolved.[8-12]

Benznidazole (BZN) and nifurtimox (NFX) were discovered more than 45 years ago and are the only drugs prescribed to treat Chagas disease (CD).[13-14] Additionally, BZN is considered as the current drug of choice because it has a better safety profile and efficacy. In the acute phase and during congenital transmission, both drugs produce a parasitological cure if they are administered soon after infection. However, in the chronic phase and disease reactivation, their efficiencies are variable. Furthermore, treatment with these drugs has important drawbacks, including lengthy treatment, severely toxic side effects and different susceptibilities against *T. cruzi* strains that can lead to treatment failure.[7, 15-18] In the last decade, different research groups have been identified potential agents to treat this parasitosis.[19-25] Interestingly, posaconazole and E1224 (ravuconazole prodrug) triggered a great expectation about their antiparasitic profile, however, clinical trials results confirmed the superiority of BZN over these candidates.[26-30] Therefore, further research is needed for the discovery of more effective and safer antichagasic agents.

Superoxide dismutase (SOD) metalloenzymes play crucial roles in antioxidant defense in aerobic organisms.[31] According to their metal selectivity, the following four isoforms have been identified: iron-SOD (Fe-SOD), copper/zinc-SOD (Cu/Zn-SOD), manganese-SOD (Mn-SOD) and nickel-SOD (Ni-SOD). An Fe-SOD isoform is found in trypanosomatids, some protozoan parasites and plants.[32-33] A Cu/Zn-SOD isoform is found in humans and mammalian hosts.[34] Due to the biochemical and structural differences that Fe-SOD presents with respect to its human ortholog Cu/Zn-SOD, it is considered a potential therapeutic target for the treatment of CD.[34]

An attractive scaffold for new antiparasitic agents are Mannich base derivatives because of their potential biological activity against different parasites responsible for tropical diseases such as

ACCEPTED MANUSCRIPT

trypanosomiasis, leishmaniasis, and malaria.[34-39] Hence, our research group has investigated a variety of Mannich base molecules, finding promising trypanocidal candidates for further preclinical studies.[40-41] Moreover, we confirmed the Fe-SOD enzyme as the main target for these derivatives which showed high selectivity compared to the human Cu/Zn-SOD ortholog. By using molecular docking, we were able to propose a binding mode for the target, suggesting that the carbonyl group, piperazine and its linked phenyl ring would be the most important scaffolds for binding this enzyme **(Figure 1)**.[40] Nonetheless, our results suggest that the presence of small *para*-substituents with either donor or acceptor hydrogen bond properties on the aromatic ring next to the carbonyl group may improve binding via interactions with Gln72. Finally, the literature reveals that Mannich bases containing amines in their structure, such as phenethylamines[42] or anilines,[43] confer anti-parasitic and anti-bacterial activity, respectively.

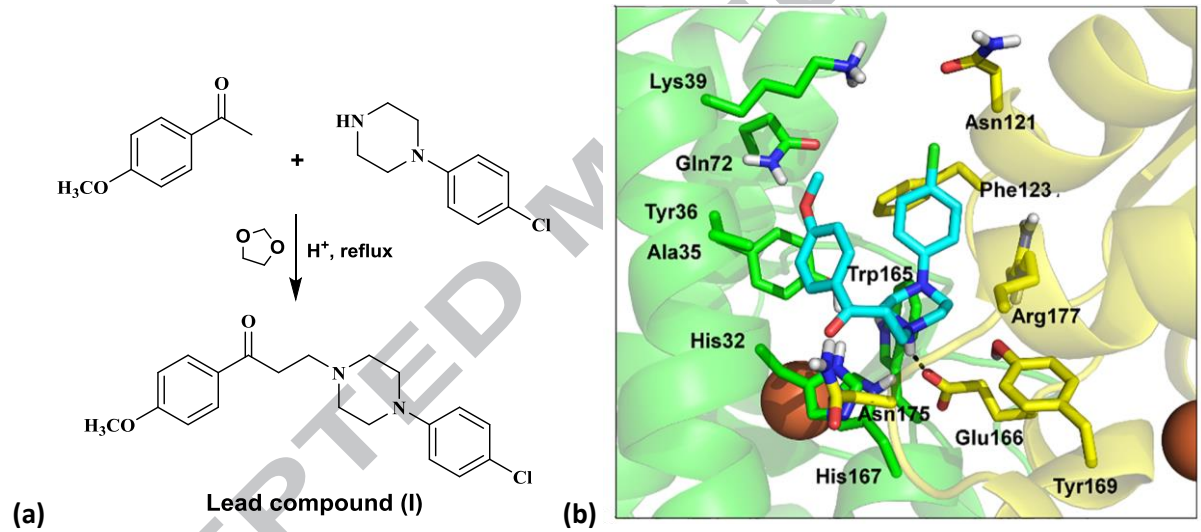


**Figure 1.** Lead compound (**I**) from Martin-Escolano *et al*[40], **(a)** Chemical synthesis and **(b)** docking results showing the binding mode of the compound to Fe-SOD enzyme (PDB ID 4DVH). Oxygen (red), nitrogen (blue), and chlorine (green).

Based on these premises, ten new derivatives were designed, starting from our previous lead compound (compound **I** in **Figure 1**), and taking into account the following strategy. Derivatives **1-6** were prepared by conserving the *para*-methoxy substituent in the aromatic ring linked to the carbonyl group **(Scheme 1)** but substituting the piperazine by different amines (phenethylamine or aniline). Furthermore, different substituents were attempted in this second aromatic group to investigate their effects on pharmacological activity. The other group of derivatives (**7-10**) were synthetized by replacing the methoxyl group in lead compound **I** to a hydroxyl group and retaining the piperazine linked to the aromatic ring **(Scheme 1)**, substituted in the *para* position by F, Cl, $CF_3$ or $NO_2$. This design, as well as the previously designed

ACCEPTED MANUSCRIPT

derivatives, takes into consideration the priority of using simple and cost-effective synthetic routes to obtain new compounds to combat this parasitic illness.

Herein, we report the synthesis and biological evaluation of ten Mannich base derivatives, which represent an interesting therapeutic alternative against this parasitosis. Additionally, the study of the possible mechanism of action was carried out for the most potent compounds.

## 2. Results and discussion

### *2.1. Chemistry*

The general reaction pathways towards Mannich base derivatives are outlined in **Scheme 1**. Vinyl ketone **i1** was prepared by the α-methylenation of 4'-methoxyacetophenone using an ammonium catalyst in THF as described by Bugarin *et al.*[44] Compounds **1-6** were synthesized via the Michael addition reaction, in which vinyl ketone (**i1**) will undergo a Michael addition with the corresponding aryl amine. Compounds **7-10** were synthesized by the Mannich reaction based on our previous experience[41] and published literature,[45-46] where 4'-hydroxyacetophenone was condensed with the corresponding arylamine in acidic medium using 1,3-dioxolane instead of paraformaldehyde and as a solvent. All new derivatives were fully characterized by IR spectroscopy and NMR ($^1$H and $^{13}$C) as well as elemental microanalysis (C, H, N).

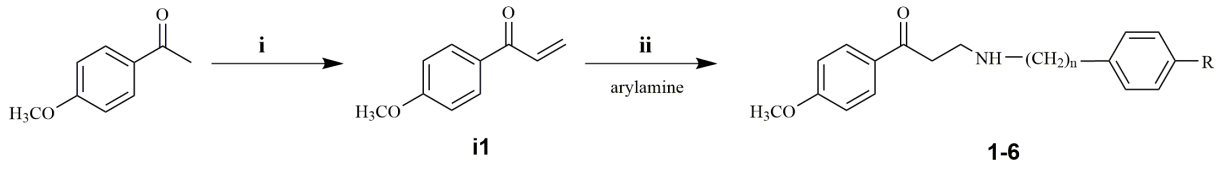


| | n | R | | n | R |
|---|---|---|---|---|---|
| **1** | 0 | $CF_3$ | **6** | 2 | Cl |
| **2** | 0 | F | **7** | - | $CF_3$ |
| **3** | 0 | Cl | **8** | - | F |
| **4** | 2 | $CF_3$ | **9** | - | Cl |
| **5** | 2 | F | **10** | - | $NO_2$ |

**Scheme 1**. General procedure for the synthesis of compounds 1-10. Reagents and conditions: (i) paraformaldehyde, diisopropylammonium trifluoroacetate, trifluoroacetic acid, THF, reflux, 8 h, (ii) $CH_2Cl_2$, rt, from 24 to 48 h; (iii) 1,3-dioxolane, HCl, reflux, 20 to 40 min.

### *2.2. In vitro assessment*

Considering the genetic diversity of *T. cruzi* strains and their variable sensitivities to clinical drugs,[47-48] compounds **1-10** and BZN, as the reference drug, were evaluated against three different strains of *T. cruzi* (Arequipa, SN3 and Tulahuen strain) belonging to different discrete

ACCEPTED MANUSCRIPT

type units (DTUs) mainly associated with this human parasitosis. Additionally, the effect on the growth and viability of host cells for *T. cruzi* was assessed using mammalian Vero cells.

The preliminary screening started with the *in vitro* evaluation of all compounds and BZN facing up to the extracellular epimastigote forms. Additionally, mammalian cell cytotoxicity assays were performed as described in the Experimental section. The results of these assays are expressed as the concentration required to inhibit 50% of the parasites or mammalian cells growth ($IC_{50}$). Likewise, the selectivity index (SI) was calculated as follows: SI = $IC_{50}$ Vero cells/$IC_{50}$ epimastigote forms. The results are summarized in **Table 1**. Compounds with an SI higher than 5 in at least two *T. cruzi* strains progressed to the *in vitro* screening in amastigote and trypomastigote forms of the parasite.

**Table 1.** *In vitro* activity of the studied compounds (**1-10**) in epimastigote forms.

| Comp | Activity $IC_{50}$ (µM)[a] | | | Toxicity $IC_{50}$ | Selectivity Index[c] | | |
|---|---|---|---|---|---|---|---|
| | Arequipa | SN3 | Tulahuen | Vero Cell (µM)[b] | Arequipa | SN3 | Tulahuen |
| **BZN** | 26.2 ± 7.3 | 15.3 ± 1.9 | 25.3 ± 0.9 | >200 | >7.6 | >13.1 | >7.9 |
| **1** | 17.8 ± 7.0 | 76.1 ± 20.3 | 24.6 ± 13.1 | 32.6 ± 7.0 | 1.8 | 0.4 | 1.3 |
| **2** | 14.8 ± 2.6 | 25.4 ± 8.2 | 14.4 ± 7.7 | 133.4 ± 6.0 | 9.0 | 5.2 | 9.3 |
| **3** | 18.7 ± 14.4 | 38.4 ± 12.3 | 16.4 ± 5.9 | 145.7 ± 22.4 | 7.8 | 3.8 | 8.9 |
| **4** | 59.7 ± 22.1 | 13.2 ± 0.9 | 13.2 ± 2.6 | 91.1 ± 2.5 | 1.5 | 6.9 | 6.9 |
| **5** | 35.6 ± 6.1 | 16.9 ± 1.0 | 20.3 ± 5.5 | 66.2 ± 4.6 | 1.9 | 3.9 | 3.3 |
| **6** | 51.6 ± 8.9 | 14.6 ± 4.2 | 15.2 ± 2.7 | 53.5 ± 4.4 | 1.0 | 3.7 | 3.5 |
| **7** | 22.7 ± 1.4 | 12.6 ± 2.2 | 14.8 ± 7.9 | 106.9 ± 11.0 | 4.7 | 8.5 | 7.2 |
| **8** | 24.4 ± 9.5 | 10.1 ± 0.6 | 13.0 ± 1.6 | 50.0 ± 5.3 | 2.1 | 5.0 | 3.9 |
| **9** | 18.6 ± 5.9 | 12.1 ± 0.9 | 10.6 ± 0.9 | 103.7 ± 10.6 | 5.6 | 8.6 | 9.8 |
| **10** | 24.8 ± 3.5 | 13.0 ± 1.1 | 43.0 ± 8.1 | 34.6 ± 11.2 | 1.4 | 2.7 | 0.8 |

$IC_{50}$: Compound concentration that reduces the number of parasites or cells growth by 50%, calculated through Graphpad prism 7 software. Results are presented as the mean and the standard deviation (SD),

ACCEPTED MANUSCRIPT

correspond to triplicates from three independent experiments. Compounds screened against *T. cruzi* epimastigotes had $r^2$ values > 0.7. (a) $IC_{50}$ values against *T. cruzi* epimastigote forms. (b) $IC_{50}$ Vero cells cytotoxicity. (c) Selectivity index (SI) corresponds to the ratio of $IC_{50}$ values of compounds against Vero cells relative to those against *T. cruzi* epimastigote forms.

Therefore, compounds **2-4**, **7** and **9** were selected to determine the $IC_{50}$ values and their respective SIs in the amastigote and trypomastigote forms **(Table 2** and **Table 3)**. The criteria established for this screening as the cut-off of this step were the same as those according to the literature[49-51]: $IC_{50}$ values approximately 10 µM and SI > 50 in at least two strains and one parasitic form. Compounds **7** and **9** met these criteria, with $IC_{50}$ values ranging from 0.7 - 6.2 µM in both amastigote and trypomastigote forms and SI > 50 in the trypomastigote forms of two *T. cruzi* strains. It is interesting to note that the lead compounds **7** and **9** contain an aryl piperazine and a hydroxyl group in the *para* position of the aromatic ring linked to the ketone group.

Therefore, more exhaustive assessments of their trypanocidal activity and genotoxic capacity were performed.

**Table 2.** *In vitro* activity of the compounds **2-4, 7** and **9** in both amastigote and trypomastigote forms of *T. cruzi*.

| **Comp.** | **Activity $IC_{50}$ (µM)** | | | | | |
|---|---|---|---|---|---|---|
| | ***T. cruzi* Arequipa strain** | | ***T. cruzi* SN3 strain** | | ***T. cruzi* Tulahuen strain** | |
| | **Amastigote forms** | **Trypomastigote forms** | **Amastigote forms** | **Trypomastigote forms** | **Amastigote forms** | **Trypomastigote forms** |
| **BZN** | 3.0 ± 0.4 | 6.2 ± 1.7 | 4.4 ± 0.2 | 33.3 ± 1.6 | 3.9 ± 0.2 | 6.7 ± 1.0 |
| **2** | 4.7 ± 1.0 | 2.1 ± 0.2 | 5.4 ± 1.6 | 3.4 ± 0.8 | 6.7 ± 0.1 | 2.7 ± 0.4 |
| **3** | 7.3 ± 1.3 | 13.0 ± 3.5 | 6.0 ± 0.6 | 63.0 ± 12.3 | 26.3 ± 0.7 | 14.2 ± 1.7 |
| **4** | 9.1 ± 0.8 | 3.6 ± 1.1 | 4.5 ± 0.4 | 5.5 ± 2.1 | 3.3 ± 0.1 | 3.5 ± 0.7 |
| **7** | 6.2 ± 0.3 | 0.9 ± 0.1 | 6.6 ± 0.6 | 2.1 ± 0.4 | 3.9 ± 0.4 | 2.3 ± 0.3 |
| **9** | 5.1 ± 0.5 | 0.7 ± 0.1 | 4.5 ± 0.3 | 2.0 ± 0.4 | 3.0 ± 0.3 | 2.1 ± 0.2 |

ACCEPTED MANUSCRIPT

*In vitro* activity against amastigote and trypomastigote forms, expressed as $IC_{50}$. Data presented as mean ± standard deviation (SD) of triplicates and at least two independent assays. Compounds screened against *T. cruzi* trypomastigotes and amastigotes had $r^2$ values > 0.7.

**Table 3.** Selectivity index of the compounds **2-4, 7** and **9** in both amastigote and trypomastigote forms of *T. cruzi*.

| Comp | Selectivity Index | | | | | |
|---|---|---|---|---|---|---|
| | ***T. cruzi* Arequipa strain** | | ***T. cruzi* SN3 strain** | | ***T. cruzi* Tulahuen strain** | |
| | **Amastigote forms** | **Trypomastigote forms** | **Amastigote forms** | **Trypomastigote forms** | **Amastigote forms** | **Trypomastigote forms** |
| **BZN** | >67.2 | >32.5 | >45.6 | >6.0 | >51.7 | >29.9 |
| **2** | 27.6 | 64.8 | 24.7 | 39.4 | 20.1 | 48.8 |
| **3** | 19.9 | 11.2 | 24.1 | 2.3 | 5.5 | 10.2 |
| **4** | 10.0 | 25.0 | 20.2 | 16.7 | 27.7 | 26.1 |
| **7** | 17.4 | 123.1 | 16.2 | 51.0 | 27.4 | 45.7 |
| **9** | 20.4 | 140.9 | 23.2 | 50.9 | 34.5 | 49.6 |

Selectivity index (SI = $IC_{50}$ Vero cells/$IC_{50}$ of *T. cruzi* forms).*Lead compound (**I**) from Martin-Escolano *et al.*[40]

Before the *in vivo* assessment, to obtain more information about the antichagasic activity of compounds **2-4**, **7**, and **9** as well as BZN, the infection rates in Vero cells were evaluated by counting the infected cells after 72 h of exposure to different concentrations (from 3.1 to 50 µM for compound **2-4** and **7**, and from 1.6 to 25 µM for compound **9**). The results are presented in **Figure 2**, together with the data used to determine the $IC_{50}$ of the compounds against the amastigote and trypomastigote forms.

In general, a gradual decrease in the ratio of infected cells was observed, while the concentration of the tested compounds increased. Thus, the compounds reduced the ratio of infected cells to 18% (BZN), 10% (compound **2**), 28% (compound **3**), 17% (compound **4**) and 7% (compound **7**), with respect to the ratio of infected cells at 50 µM. Compound **9** decreased the rate of infected cells to 19% and BZN to 18% at 25 µM. In addition, it is remarkable that compounds **7** and **9** showed a similar or higher infection rate at these concentrations compared to the

ACCEPTED MANUSCRIPT

reference drug. Additionally, it is important to note that compounds **2**, **7** and **9** showed the best $IC_{50}$ values in trypomastigotes, amastigotes and infected Vero cells (**Figure 2**).

Finally, considering the results of activity and selectivity in different strains, as well as the different forms and ratios of infected Vero cells, compounds **7** and **9** were selected as good candidates for the *in vivo* study. Prior to the *in vivo* evaluation, the lead compounds were evaluated to determine their genotoxic capacity.

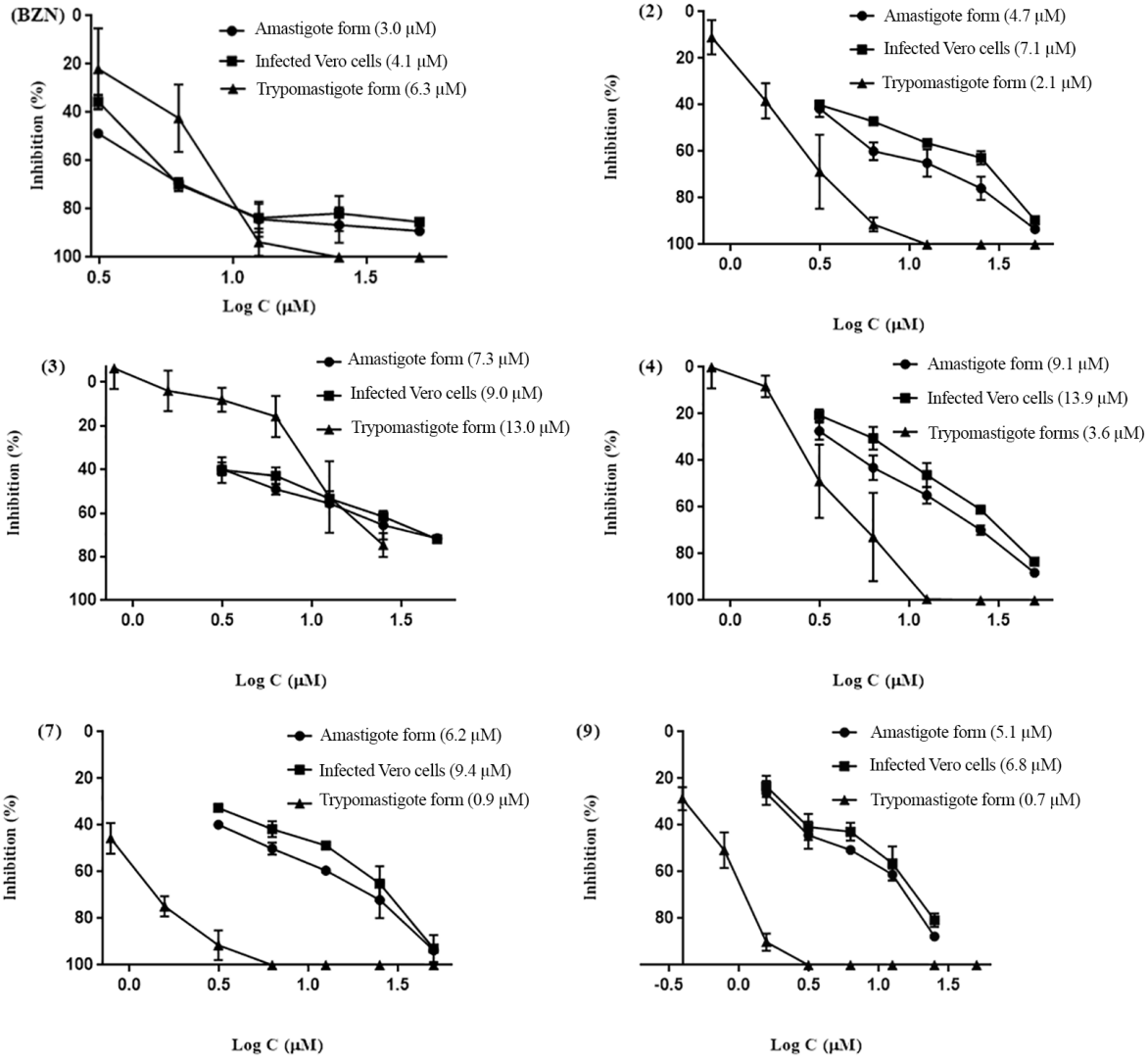


**Figure 2.** Effect of the compounds in the propagation of the amastigotes and trypomastigotes and infected Vero cells. The graphs are obtained from the mean and standard deviation of at least two independent assays. $IC_{50}$ values (in parenthesis) that were calculated using Graphpad prism 7 software.

*2.3. In vitro genotoxicity screening. SOS/UMU-test*

ACCEPTED MANUSCRIPT

This assay was conducted to investigate the potential genotoxicity of compounds **7** and **9**. The results displayed that none of our compounds were genotoxic either in the presence or absence of metabolic activation (see **S2 section** of the **supporting information**), whereas BZN induced genotoxicity under the same conditions.[41] Therefore, the results led us to examine these compounds in *in vivo* studies in BALB/c mice infected with the parasite.

*2.4. In vivo anti-T. cruzi activity in BALB/c female mice*

Compounds **7** and **9** were selected for *in vivo* assays based on encouraging results of their trypanocidal activity *in vitro*, SI and non-genotoxicity in the preliminary SOS/UMU tests. The currently used chemotherapy has variable activity in the acute and chronic phase of this disease[52]; therefore, test compounds were evaluated in both phases according to the experiments established in **Scheme 2**. First, BALB/c mice were infected intraperitoneally according to the literature.[53] Compounds **7** or **9** or BZN were administered orally, which is the route of administration ideally recommended to treat this parasitosis according to the target product profile (TPP) established by the Drugs for Neglected Diseases Initiative (DND*i*).[54] The mice were treated with the compounds from day 8 post-infection (pi), at 20 mg/kg/day for 5 consecutive days. This dosage represents a subcurative dose of BZN; therefore, this experiment demonstrates whether the studied compounds are more effective or not than the reference drug during the progress of the disease.

Parasitemia levels of different study groups during the acute phase were determined by counting bloodstream trypomastigotes as described in the experimental section. Nonsignificant differences were evidenced between the untreated mice and the mice treated with compound **7**. Compound **9** showed an antiparasitic activity similar to BZN **(Figure 3)**. Compound **9** showed lower parasitemia levels from the beginning of the treatment, and this behavior was maintained until the end of the phase (48 days pi), noting that blood parasitemia levels were reduced to undetectable levels four days before the reference drug (BZN) levels. Furthermore, it is noteworthy that, during this phase, compound **9** decreased the parasitemia peak by approximately 70% compared to the untreated control.

ACCEPTED MANUSCRIPT

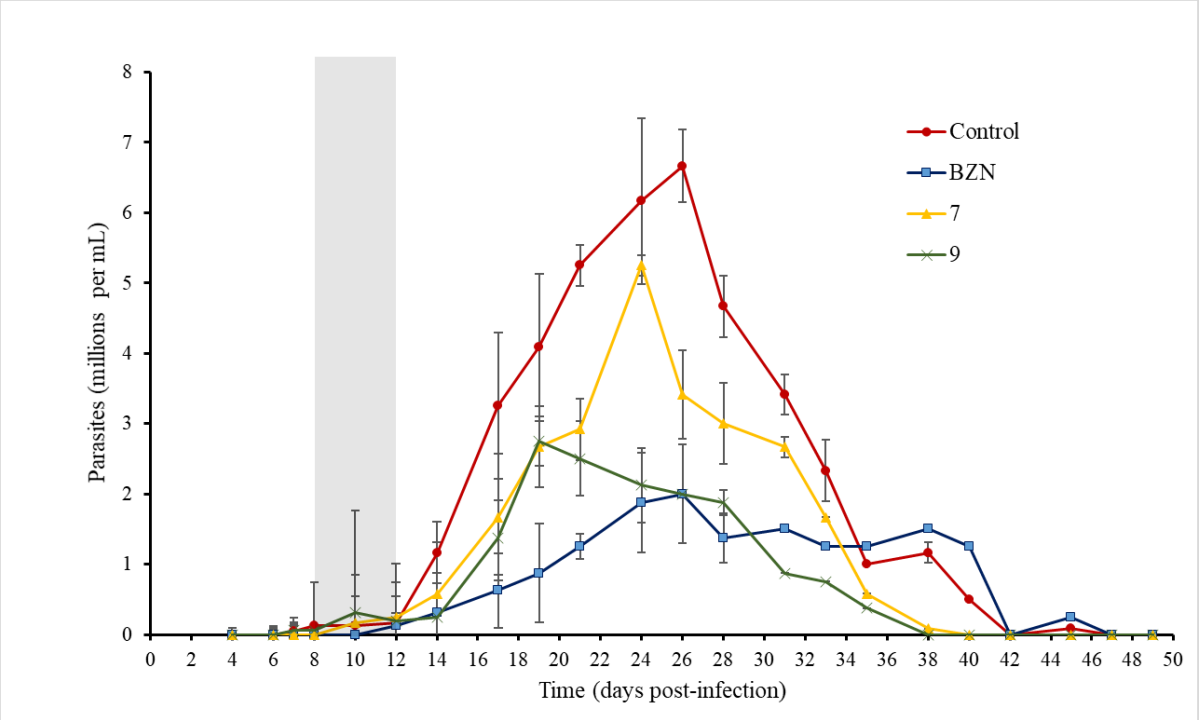


**Figure 3.** Parasitemia levels during acute phase of Chagas disease in BALB/c mice non-treated (control) and treated with compound **7, 9** and BZN. All compounds were orally administered with 20 mg/kg/day for 5 consecutive days. Days of treatment are represented in gray. Values are the means of results for three mice ± standard deviation.

On day 80 pi, the mice were immunosuppressed with cyclophosphamide to evaluate the effectiveness of the treatment; this procedure expands the residual foci of infection to detectable levels (if after being treated there was still presence of parasites in the vertebrate host).[55-56] In addition, this reactivation of parasitemia in the chronic phase has great relevance since it can occur in immunocompromised patients, where the efficacy of current chemotherapy is unknown, although it is presumed to be limited.[16, 57]

**Figure 4** shows the reactivation percentages of infection compared to those of the untreated (control) group after the mice were immunosuppressed with cyclophosphamide. As observed, mice treated with compounds **7** or **9** or BZN showed a decrease in parasitemia in both phases. The reactivation obtained in the acute phase could be proportional to the survival rate observed in the parasitemia curve (mentioned above). It is also important to note that all mice treated with the compounds in the chronic phase showed a lower percentage of reactivation than treated mice in the acute phase. It is noteworthy to mention that mice treated with compound **9** showed a reactivation of approximately 25% and 20% in the acute and chronic phases, respectively, and this compound was more effective than the reference drug (approximately 65% and 40% in the

ACCEPTED MANUSCRIPT

acute and chronic phase, respectively). Although there was a higher percentage of reactivation (approximately 85%) in the groups treated with compound **7** in the acute phase, this value decreased to 30% in the chronic phase. These results lead us to hypothesize that treatment with compound **9** could be effective for both the acute and chronic phases of CD. This effectiveness was confirmed later with the results obtained from tissue PCR.

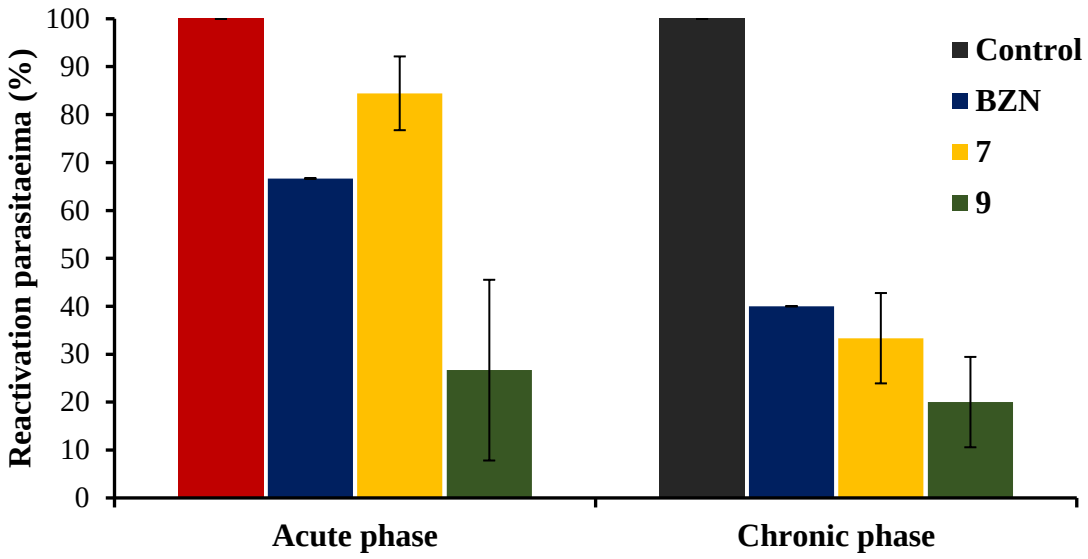


**Figure 4.** Immunosuppression experiment in the *in vivo* assay for BALB/c mice non-treated and treated with compound **7, 9** and BZN. The figure shows the reactivation parasitemia (%), after cycles administration of the immunosuppressant cyclophosphamide. Values are the means of results for three mice ± standard deviation.

In accordance with previous studies, tissue PCR in animals has better sensitivity because it can detect *T. cruzi* DNA in mice that are considered cured, as evaluated by other blood methodologies.[58] Therefore, in addition to evaluating the effectiveness of the compounds after immunosuppression, the presence of parasites in target organs was evaluated through PCR after necropsy (100 day). **Figure 5** shows the PCR results for the target organs in all studied groups in both the acute and chronic phases. Untreated mice (control group) in both phases showed the presence of parasites in all target organs/tissues: adipose, bone marrow, brain, esophageal, heart, muscle, spleen and stomach tissues. Mice treated with BZN demonstrated 25% and 38% of organs and tissues free of parasites in the acute and chronic phases, respectively. A low percentage was observed in the mice treated with compound **7** in the acute phase (13%), although 50% was obtained in the chronic phase of this compound. Notably and in accordance with the abovementioned results, compound **9** showed a better antiparasitic activity, even better

ACCEPTED MANUSCRIPT

than that of the reference drug, with 50% (acute phase) and 63% (chronic phase) of organs and tissues free of parasites, respectively.

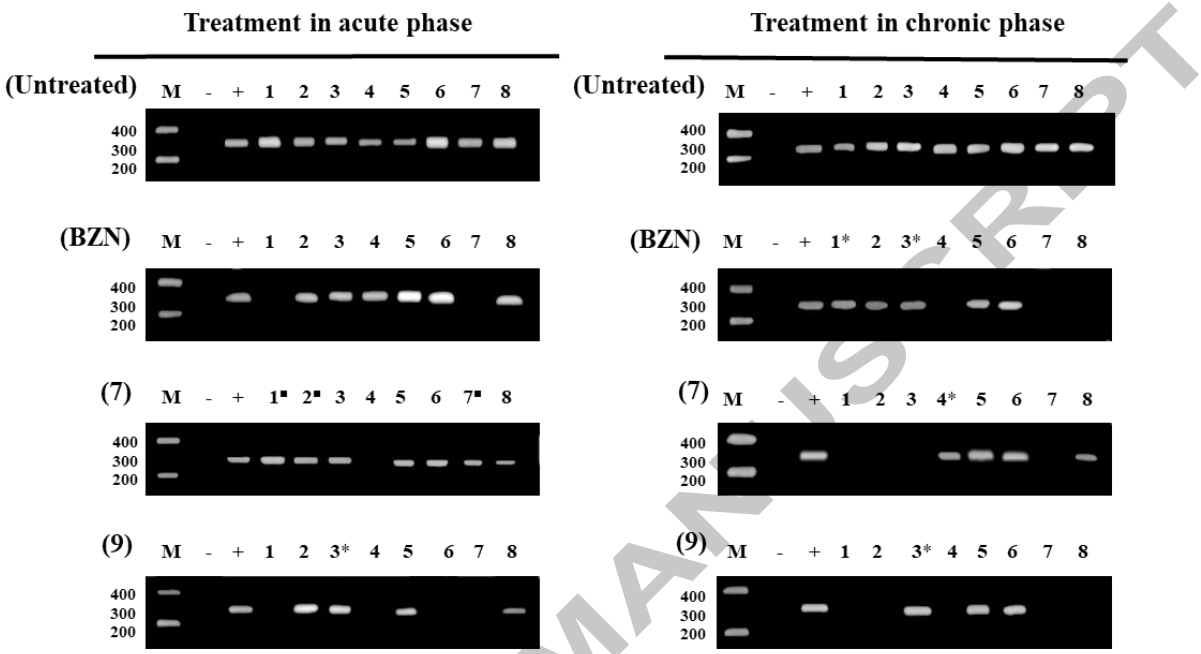


**Figure 5.** PCR analysis of 8 tissues with the *T. cruzi* splice leader (SL) gene at the final day of experiment in mice untreated and treated with 20 mg/kg/day for 5 consecutive days. Lanes: M, base pair (bp) marker; -, PCR negative control; +, PCR positive control; 1, PCR adipose tissue; 2, PCR bone marrow tissue; 3, PCR brain tissue; 4, PCR oesophagus tissue; 5, PCR heart tissue; 6, PCR muscle tissue; 7, PCR spleen tissue; 8, PCR stomach tissue. *, It means that 1/3 of the corresponding organ PCR products showed 300 bp band on electrophoresis; ▪, It means that 2/3 of the corresponding organ PCR products showed 300 bp band on electrophoresis; no * nor ▪, it means that 3/3 or 0/3 of the corresponding organ PCR products showed 300 bp band on electrophoresis.

However, the immune response to *T. cruzi* infection was evaluated by determining the levels of immunoglobulin G (IgG) via ELISA using Fe-SOD isolated in the laboratory[59] as the antigen.[60] The titer of IgG is associated with the infection ratio (parasitic load), which would allow us to evaluate the effectiveness of the studied compounds in combination with the innate protection of mice.[40, 61] **Figure 6** shows the titer of anti-*T. cruzi* IgG in the different groups and the respective controls. As observed, all treated mice, both acute and chronic, had lower levels of IgG than untreated mice (control). Mice treated with compounds **7** or **9** had mostly similar IgG values to those treated with BZN; however, during the acute phase, the efficacy of BZN was

ACCEPTED MANUSCRIPT

better than that of both compounds. These results allow us to confirm the antichagasic activity of both compounds (**7** and **9**), especially their effectiveness in the chronic phase.

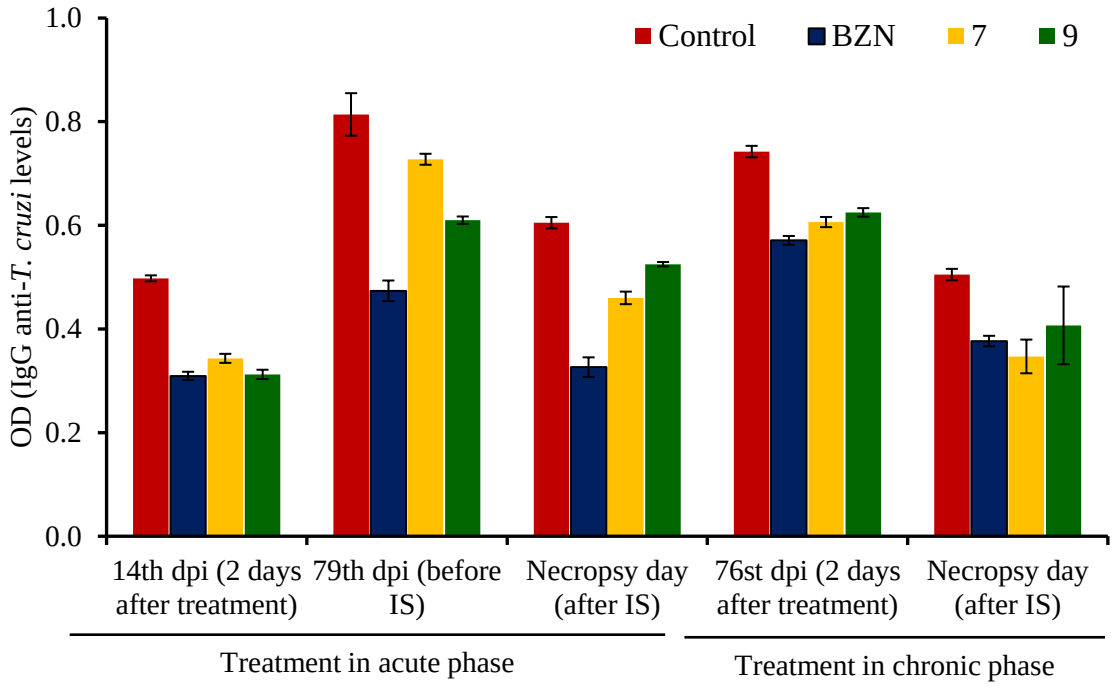


**Figure 6.** Differences in the Ig G levels of anti-*T. cruzi* antibodies, expressed in absorbance units, optical densities (OD) at 490 nm, between non-treated (control) and treated groups of mice. Values constitute means of three mice ± standard deviation.

Furthermore, splenomegaly is manifested in both phases of the infection induced by *T. cruzi*[62]; therefore, this phenomenon indicates the link between the parasitic load and the enlargement of the spleen.[40] **Figure 7** shows the weight percentage of the spleens in the different groups studied, including the nontreated and noninfected groups. The nontreated mice demonstrated an increase in the weight of the spleen of more than twice the weights of noninfected mice, ranging from 0.28% to 0.47% of the total weight of the mice. In addition, all treated mice, even at subcurative doses of BZN, demonstrated a smaller increase in the weight of the spleen compared to untreated mice, either in the acute or chronic phases, highlighting a decrease in the splenomegaly by compound **9** of 44% and 81% in the acute and chronic phases, respectively, and by compound **7** of 66% in the chronic phase compared to the reference drug. Therefore, these results were consistent with the results described above, where the tested compounds reduced the infection rates, emphasizing the antichagasic activity of compound **9**.

ACCEPTED

ACCEPTED MANUSCRIPT

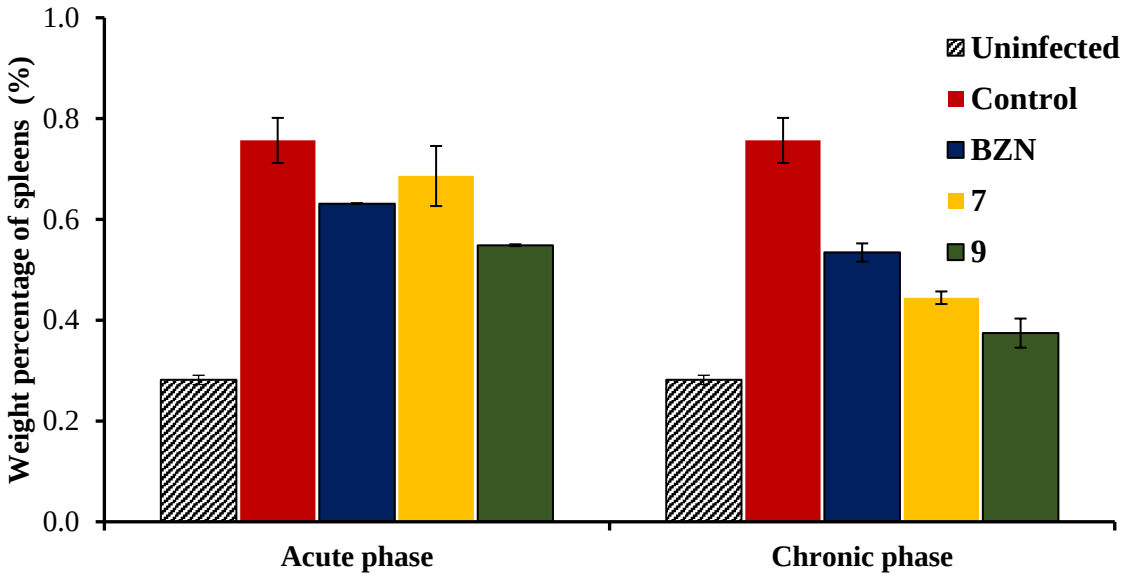


**Figure 7.** Weight percentage of spleens (%) of different groups of mice at the end of experiment. Values constitute means of three mice ± standard deviation.

ACCEPTED MANUSCRIPT

ACCEPTED MANUSCRIPT

**Table 4.** Biochemical clinical parameters of groups of Balb/c mice infected with *T. cruzi*.

| | | Kidney marker profile | | Heart marker profile | | Liver marker profile | | | |
|---|---|---|---|---|---|---|---|---|---|
| | | **Urea ($mg \cdot DL^{-1}$)** | **Uric acid ($mg \cdot DL^{-1}$)** | **CK-MB[a] ($U \cdot L^{-1}$)** | **LDH[b] ($U \cdot L^{-1}$)** | **AST/GOT[c] ($U \cdot L^{-1}$)** | **ALT/GPT[d] ($U \cdot L^{-1}$)** | **Total bilirubin ($mg \cdot DL^{-1}$)** | **Alkaline phosphatase ($U \cdot L^{-1}$)** |
| | **Uninfected mice (n = 6)** | 35 [32─40] | 4.5 [4.0─5.1] | 372 [150─630] | 3180 [2505─3851] | 153 [132─177] | 55 [46─62] | 0.28 [0.22─0.31] | 169 [141─192] |
| **Treatment in acute phase** | 14th dpi (Control) (n = 3) | 37 | 4.0 | 365 | 3285 | 177 | 45 | 0.31 | 158 |
| | 14th dpi and BZN (2 days after treatment) (n = 3) | ---- | ---- | ---- | - | ++ | ++++ | - | = |
| | 14th dpi and **7** (2 days after treatment) (n = 3) | - | --- | ---- | --- | = | ++++ | ++++ | ---- |
| | 14th dpi and **9** (2 days after treatment) (n = 3) | -- | - | ---- | --- | - | ++++ | + | -- |
| | Necropsy day of mice (Control) (n = 3) | 33 | 4.4 | 528 | 3809 | 156 | 64 | 0.30 | 176 |
| | Necropsy day of mice and BZN (n = 3) | --- | -- | = | + | + | = | = | = |
| | Necropsy day of mice and **7** (n = 3) | = | ---- | ---- | = | = | = | ++++ | ---- |
| | Necropsy day of mice and **9** (n = 3) | -- | = | --- | = | = | ++ | = | - |
| **Treatment in chronic phase** | 76th dpi (Control) (n = 3) | 35 | 4.6 | 505 | 3166 | 188 | 58 | 0.25 | 164 |
| | 76th dpi and BZN (2 days after treatment) (n = 3) | --- | ---- | ---- | -- | + | ++++ | - | = |
| | 76th dpi and **7** (2 days after treatment) (n = 3) | = | --- | ---- | --- | -- | ++++ | ++++ | -- |
| | 76th dpi and **9** (2 days after treatment) (n = 3) | ---- | = | ---- | - | -- | + | - | = |
| | Necropsy day of mice (Control) (n = 3) | 33 | 4.4 | 528 | 3809 | 156 | 64 | 0.30 | 176 |
| | Necropsy day of mice and BZN (n = 3) | ---- | ---- | - | -- | = | = | - | - |
| | Necropsy day of mice and **7** (n = 3) | = | -- | ---- | ---- | = | = | ++ | ---- |
| | Necropsy day of mice and **9** (n = 3) | - | = | --- | = | -- | = | -- | = |

[a] CK-MB, creatine kinase-muscle/brain. [b] LDH, lactate dehydrogenase. [c] AST/GOT, aspartate aminotransferase. [d] ALT/GPT, alanine aminotransferase. dpi = day post-infection.

Key: =, variation no larger than 10 %; +, up to 10 % increase over the range; ++, up to 20 % increase over the range; +++, up to 30 % increase over the range; ++++, more than 40 % increase over the range; −, up to 10 % decrease over the range; − −, up to 20 % decrease over the range; − − −, up to 30 % decrease over the range; − − − −, more than 40% decrease over the range.

ACCEPTED MANUSCRIPT

Finally, biochemical parameters were tested to evaluate the possible metabolic abnormalities related to treatment. According to the results summarized in **Table 4**, biochemical parameters in groups treated with compounds **7** or **9** were less altered than those in the group treated with the reference drug. However, the biochemical results obtained from necropsy showed that most of these alterations returned to normal levels, with approximately 50% of the values obtained in both phases (acute and chronic). With the encouraging results obtained in the *in vivo* experiment, we could consider compound **9** as a potential candidate to treat both phases of the illness. In addition, these results allow us to consider compound **7** for further studies of combined treatment due to its antiparasitic activity in the chronic phase. In addition, considering the activity and cytotoxicity values, although compound **9** is more cytotoxic than compound **I**, the $IC_{50}$ values against different *T. cruzi* strains and forms are similar.

*2.5. Studies of the mechanism of action*

*2.5.1. Metabolite excretion*

It is known that, for energy generation, *T. cruzi* requires a high rate of glucose consumption. This parasite, which is produced and excreted into medium, reduces catabolites such as pyruvate, acetate, and succinate, which are products of glucose catabolism, even under aerobic conditions, instead of completely degrading glucose to $CO_2$ and water.[63-66] $^1$H-NMR spectra show the presence of these catabolites in fermentative medium.[65] Therefore, epimastigote forms of the *T. cruzi* Arequipa strain, untreated or treated with compounds **7** or **9** or BZN, were analyzed by this technique to compare the effect of these compounds on glucose catabolism at $IC_{50}$ concentrations. **Figure 8** shows the percentage variation among peaks of excreted catabolites in treated parasites compared with that in nontreated parasites. As observed, the excretion of all metabolites was altered in the treatment groups, with succinate being the most altered metabolite, with values from more than 30% of variation with respect to the control group. Compound **7** caused a remarkable decrease in succinate excretion (~ 80%). To avoid an energy deficit, other glycolytic routes could have been activated, producing a greater amount of pyruvate to obtain acetate, D-lactate, ethanol and L-alanine as final products. Additionally, the glycerol pathway could be activated.[66] Thus, an increase in these metabolites was detected in the medium by $^1$H-NMR. In contrast, in **9**-treated parasites, a remarkable increase in excreted succinate and pyruvate was found of 34% and 36%, respectively. A significant variation in excreted succinate was also found in BZN. According to previous studies, an increase in excreted succinate may be related to mitochondrial dysfunction.[66-67] For this reason, mitochondrial assays were performed.

ACCEPTED MANUSCRIPT

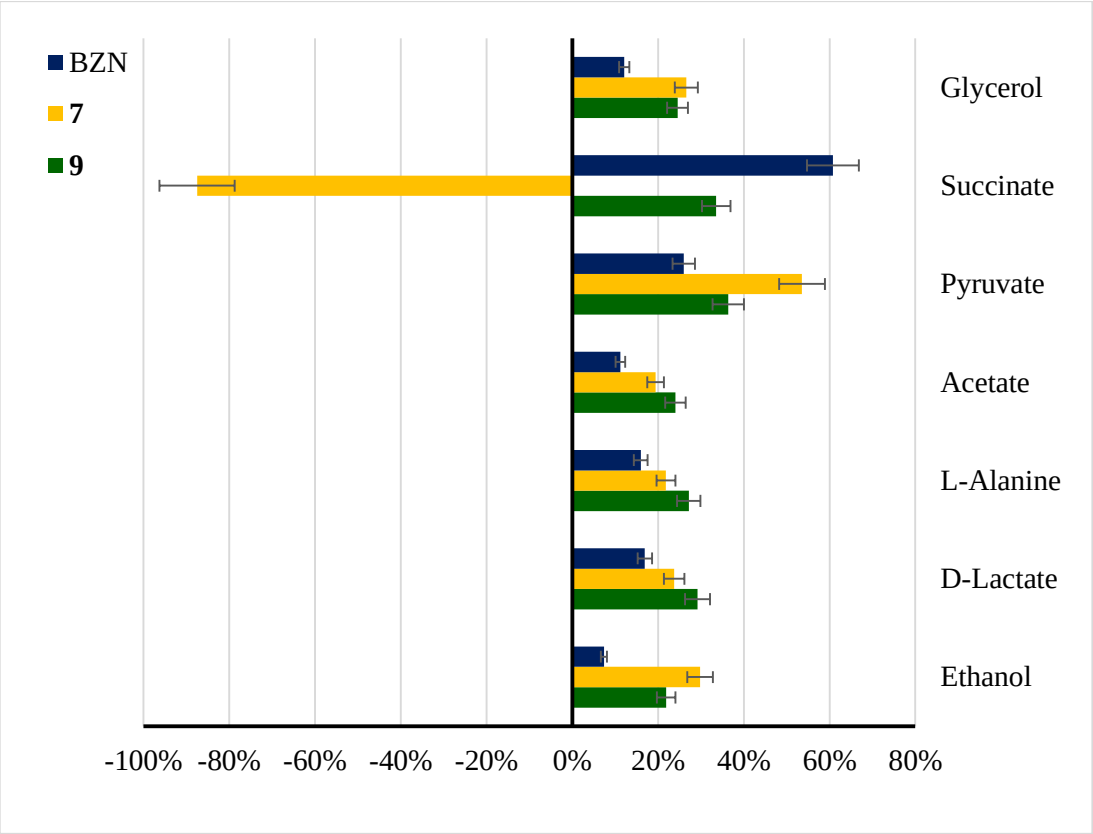


**Figure 8.** Variation (%) among peaks of catabolites excreted by epimastigote forms of *T. cruzi* Arequipa strain exposed to compound **7, 9** and BZN at $IC_{50}$ concentrations in comparison to untreated parasites incubated 72 h.

*2.5.2. Mitochondrial membrane potential*

Mitochondria play important roles in cell sustenance preservation. One of tasks of mitochondria is the maintenance of an electrochemical gradient through the inner membrane. Disturbances in membrane potential could generate a decrease in ATP levels as well as less DNA replication and RNA transcription, leading to cell apoptosis and/or necrosis.[68-69]

Therefore, to continue with the metabolite excretion studies, where a possible mitochondrial malfunction was found, probably due to an alteration in the glycolytic pathway, rhodamine 123 (rho 123) and acridine orange (AO) staining were performed to evaluate the function and integrity of this organelle by flow cytometry.[40] **Figure 9** summarizes the percentage variation obtained after the evaluation of the membrane potential. As shown, there was a reduction in the mitochondrial membrane potential in parasites treated with BZN (15.2%), which can be attributed to its mechanism of action.[70] Compound **7**-treated parasites reached a mitochondrial membrane depolarization of 54.4%, while parasites treated with compound **9** reached the highest depolarization (67.6%). Therefore, these results suggest that the trypanocidal activity of compounds **7** and **9** may be related to an effect at the mitochondrial level.

ACCEPTED MANUSCRIPT

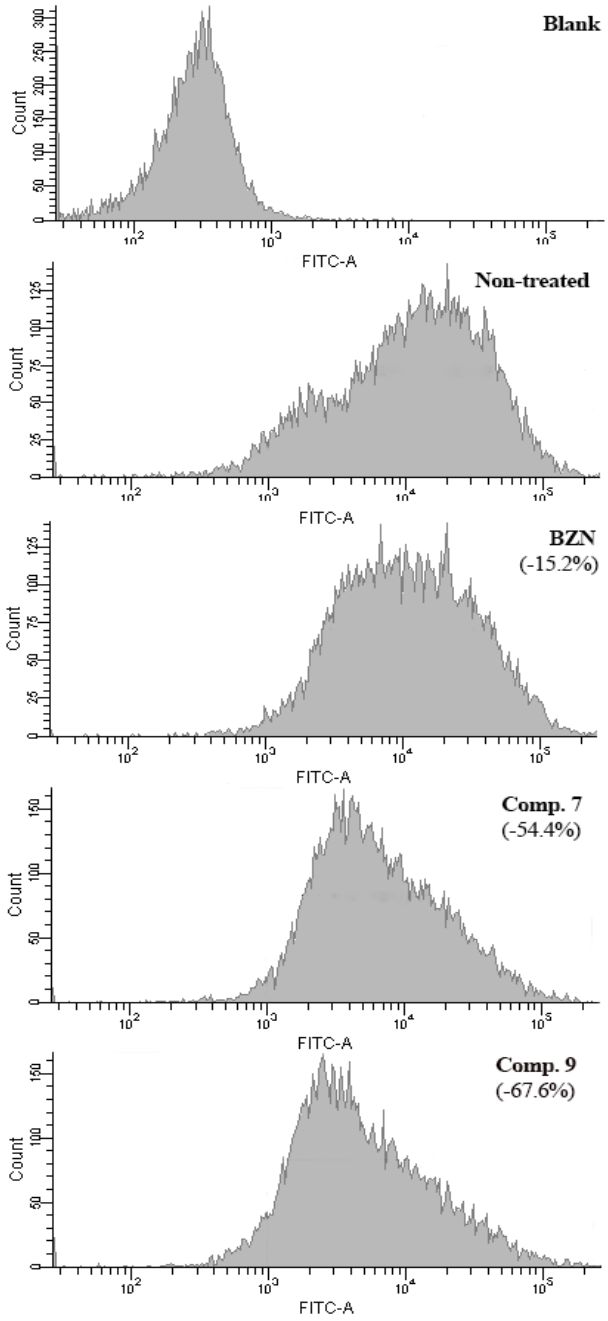


**Figure 9.** Cytometry analysis of the mitochondrial membrane potential from epimastigote forms of *T. cruzi* Arequipa strain exposed to BZN and compounds **7** and **9** at their $IC_{50}$ in comparison to non-treated parasites incubated 72 h. Percentage of variation in mitochondrial membrane potential in parenthesis.

*2.5.3. DNA and RNA levels*

The alteration of the mitochondrial membrane potential induces a decrease in ATP levels and generates an imbalance in the NADH/$NAD^+$ ratio,[66] affecting DNA replication and RNA transcription in parasitic genes. Therefore, DNA and RNA levels were quantified by flow cytometry, employing AO as the fluorescent dye. The percentage change results are shown in

ACCEPTED MANUSCRIPT

**Figure 10.** Nonsignificant differences were observed among the parasites treated with BZN, **7** or **9** and the nontreated parasites.

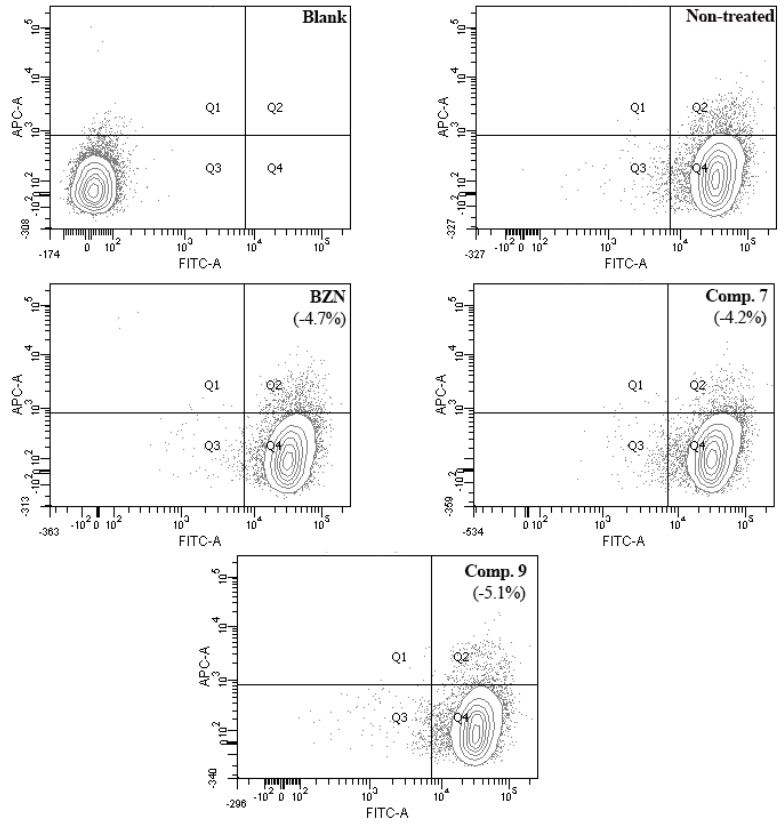


**Figure 10.** Flow cytometry analysis of the inhibition in DNA and RNA levels of epimastigote forms of *T. cruzi* Arequipa strain exposed to compound **7, 9** and BZN at their $IC_{50}$ in comparison to control parasites incubated during 72 h**.** Percentage change at DNA and RNA levels in parenthesis.

*2.5.4. T. cruzi Fe-SOD enzyme*

Previous studies from our research group showed the selective inhibitory capacity of these Mannich base derivatives on Fe-SOD and their possible binding mode for this enzyme by computational studies.[40-41] Therefore, inhibition studies of compounds **7** and **9** were carried out on Fe-SOD and Cu/Zn-SOD enzymes to determine their selective potential inhibition against the enzyme present in the parasite.

**Figure 11** shows the inhibition curve of compounds **7** and **9**, with the corresponding $IC_{50}$ of Fe-SOD from epimastigote forms of the Arequipa *T. cruzi* strain and its human homologue Cu/Zn-SOD from erythrocytes (Sigma-Aldrich). As observed in **Figure 11**, compounds **7** and **9** showed a significant inhibitory capacity for the Fe-SOD enzyme, whereas an inhibitory effect by the human enzyme was not detected up to a 50 µM concentration. Both tested compounds (**7** and **9**) reached more than 50% inhibition of Fe-SOD at a 6.3 µM concentration with $IC_{50}$

ACCEPTED MANUSCRIPT

values of 4.3 and 3.9 µM, respectively. It is noteworthy to mention that compound **7** reached total inhibition at a concentration of 25 µM. Hence, a remarkable selective inhibition of compounds **7** and **9** against Fe-SOD allows us to propose this enzyme as a possible target of action of these agents. Moreover, the significant variation in metabolites or these compounds (**Figure 8**) may be due to the inhibition of the Fe-SOD enzyme, generating oxidative stress and final damage of the parasite. However, we should not rule out other secondary routes of action for our compounds.

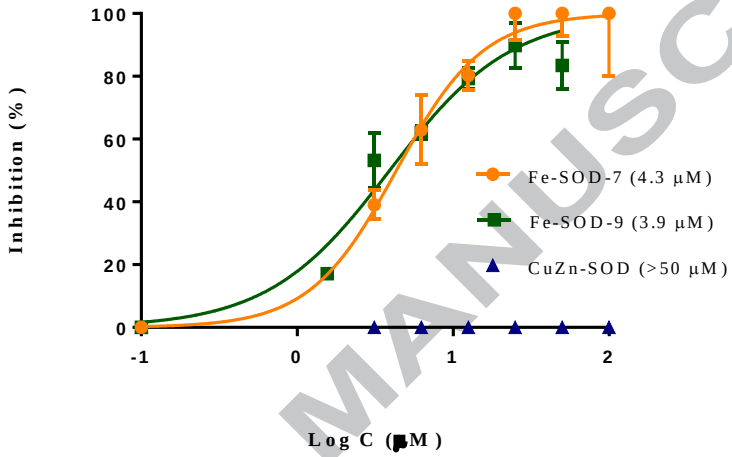


**Figure 11.** *In vitro* inhibition of Fe-SOD (activity 32.3 ± 6.7 U/mg) and CuZn-SOD (activity 781.5 ± 3.0 U/mg) for compounds **7** and **9**. Values are the mean of three independent determinations ± standard deviation. In brackets: $IC_{50}$ value that were calculated using Graphpad prism 7 software.

### *2.6. Mutagenicity assay*

#### *2.6.1. Ames test*

Considering the promising results obtained from the biological assays of the compound **9**, prompted us to evaluate its mutagenic capacity. Though the compound was negative in the SOS/UMU test, it is known that some compounds can induce mutations without activating the SOS pathway.[71] In order be sure about the safety of compound **9**, a miniaturized version of the Ames test, using 6 well plates, was performed following the principles of the OECD guideline for the Ames test.[72] The highest concentration tested, 600 µg/well, was determined in a previous solubility study. Results showed that compound **9** was not mutagenic in the presence or the absence of external metabolic activation and in any of the strains used (**Table 5**). The compound **9** was toxic in some of the conditions tested. At this stage, when comparing the toxicological results obtained from compound **9** with the published reports about BZN and NFX,[73-75] in which positive results in the Ames test were reported, compound **9** seems to have a better toxicological

ACCEPTED MANUSCRIPT

profile. Therefore, the results led us to consider the compound **9** as an interesting candidate for further preclinical studies.

**Table 5.** Results of the Ames test

| | Mean number of relevant colonies/well (Mean ± SD of 3 wells) | | | | | | | | | |
|---|---|---|---|---|---|---|---|---|---|---|
| | **TA97a** | | **TA98** | | **TA 100** | | **TA 102** | | **TA1535** | |
| | **-S9** | **S9** | **-S9** | **S9** | **-S9** | **S9** | **-S9** | **S9** | **-S9** | **S9** |
| **Negative control** | 37 ± 6.5 | 55 ± 7.1 | 3.0 ± 2.6 | 4.0 ± 2.0 | 35.7 ± 0.6 | 47.3 ± 5.7 | 78.7 ± 7.8 | 72.0 ± 1.0 | 13.3 ± 2.5 | 5.0 ± 3.6 |
| **Test dose (µg/plate)** | | | | | | | | | | |
| **7.4** | 34.4 ± 5.0 | 44.3 ± 6.8 | 4.0 ± 1.7 | 6.0 ± 1.0 | 32.3 ±1.5 | 44.7 ± 2.3 | 72.0 ± 5.0 | 75.0 ± 5.0 | 2.3 ± 0.6 | 5.5 ± 0.7 |
| **22.2** | 35.7 ± 1.2 | 38.3 ± 4.5 | 4.7 ± 0.6 | 4.0 ± 1.7 | 34.3 ± 5.8 | 47.3 ± 5.1 | 69.7 ± 2.5 | 84.7 ± 7.6 | 4.0 ± 2.0 | 3.0 ± 1.0 |
| **66.7** | 31.3 ± 5.7 | 44.0 ± 7.0 | 4.0 ± 0.0 | 6.3 ± 0.6 | 38.0 ± 3.6 | 54.7 ± 5.9 | 73.3 ± 4.0 | 72.3 ± 0.6 | 3.7 ± 2.3 | 3.3 ± 0.6 |
| **200.0** | 32.3 + 8.3 | 41 ± 2.6 | tox[a] | 2.7 ± 1.2 | tox | 42.3 ± 6.7 | tox[a] | 78.0 ± 12.3 | 4.0 ± 1.7 | 7.0 ± 2.0 |
| **600.0** | tox[a] | tox[a] | tox[a] | tox[a] | tox[a] | tox[a] | tox[a] | tox[a] | tox[a] | tox[a] |
| **Positive Control** | 196.0 ± 7.2 | 242.0 ± 35.2 | 238.7 ± 18.0 | 289.3 ± 25.7 | 225 ± 15.0 | 319 ± 12.2 | 261.3 ± 40.9 | 133.7 ± 1.2 | 235.3 ± 31.3 | 96.0 ± 7.2 |

[a] Tox = Toxicity

Before to docking studies, it is interesting to note that, throughout the *in vitro* and *in vivo* evaluation, compound **9** has shown an interesting antiparasitic profile and although the cytotoxicity values are higher than BZN and lead compound **I**, it has an encouraging safety profile.

*2.7. Docking study of the new compounds on the T. cruzi Fe-SOD enzyme*

To study the binding mode of the new compounds and to observe if it agrees with the hypotheses

ACCEPTED MANUSCRIPT

used for their rational design, we performed docking studies for all ten derivatives on the Fe-SOD enzyme. Our results suggest a binding mode similar to that of our previous series (**Figure 1b**).[40-41] The full docking results can be found as supplementary information (**Supporting information Figure S3.1**). In **Figure 12**, we show the proposed binding mode for compounds **7** and **9**, where we can observe possible hydrogen bonds between: i) the compound carbonyl group and both His32 and Tyr36, and ii) the new hydroxyl group proposed in our design strategy and Gln72. Therefore, the inclusion of hydrogen bond donors substituted in *para* in the aromatic ring next to the carbonyl group may actually increase the affinity of compounds by allowing interactions with Gln72. Also, electrostatic interactions are observed between the amino acid Lys39 (and for some compounds also Asn121), and the substituent in *para* in the other aromatic ring (the one bound to the piperazine scaffold). Similar interactions are observed for compounds **7** to **10**. For compounds **1-6**, our results suggest that the substitution of a piperazine by phenethylamines or anilines may modify the binding mode of the compounds on the dimer interface. Those compounds are expected to bind in an inversed conformation, where the aromatic scaffolds will still bind between Phe123 and Tyr36, and the carbonyl group could perform hydrogen bonds with Lys39 (**Supporting information Figure S3.1**). This agrees with the good activity observed for them (**Table 1**).

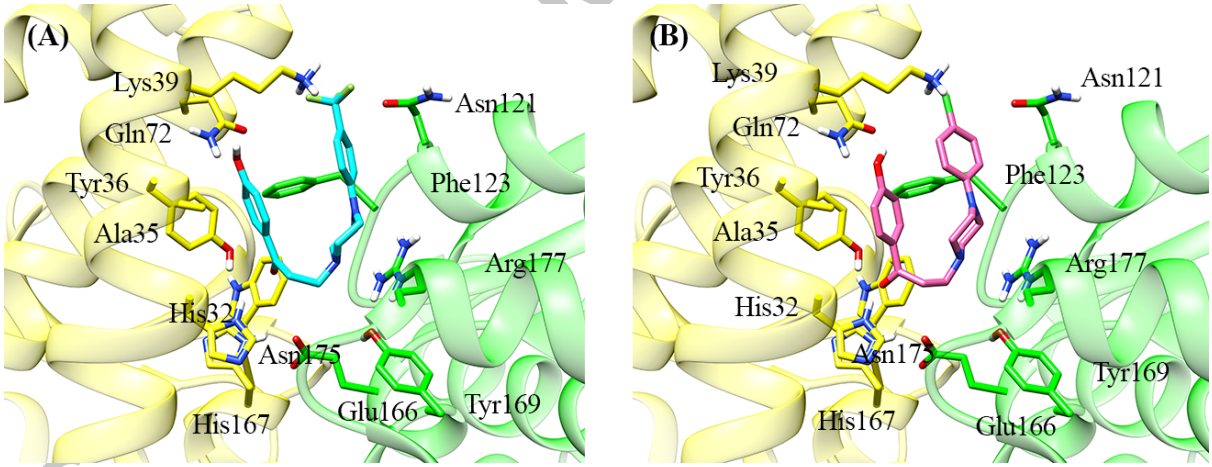


**Figure 12.** Lowest scored binding pose obtained for compounds **7** (**A**) and **9** (**B**) by molecular docking on the Fe-SOD enzyme (PDB ID 4DVH),[76] showing the compounds bound at the dimer interface. The figures were created with the software chimera.[77] Non-polar hydrogen atoms are not displayed. The following color scheme was used: protein chain A in yellow and chain B in green, compound **7** in cyan and compound **9** in pale pink.

## 3. Conclusion

In conclusion, a series of ten Mannich base-type derivatives were rationally designed, synthesized, characterized and evaluated for their antichagasic activity. The *in vitro* assays allowed us to select compounds **7** and **9** based on activity, selectivity and non-genotoxicity for

ACCEPTED MANUSCRIPT

*in vivo* testing in both the acute and chronic phases of Chagas disease. After performing different assays, such as PCR and immunosuppression, both compounds were of interest because they both caused a substantial decrease in parasitemia in the chronic phase when compared with the reference drug. Furthermore, compound **9** also showed remarkable antichagasic activity during the acute phase. The possible mechanism of action via different assays, including metabolite excretion, mitochondrial membrane potential and the inhibition of SOD, was investigated. These *in vitro* studies demonstrated that both compounds may act by the selective inhibition of Fe-SOD. Furthermore, docking studies were done to identify the binding mode of the Fe-SOD enzyme. We found that these compounds act similarly to the previously studied series. Therefore, these results allow us to consider both compounds for further studies in the development of promising candidates in Chagas therapy.

## 4. Experimental

### *4.1. Chemistry*

#### *4.1.1. Material and methods*

All the chemicals were purchased by commercial vendors and were used without further purification. The synthesis of final compounds was followed by thin layer chromatography (TLC) using SIL G/$UV_{254}$, 0.2 mm thickness (ALUGRAM® Xtra SIL G, Macherey-Nagel GmbH & Co. KG) as the stationary phase, solvent mixtures ($CH_2Cl_2$/methanol or hexane/ethyl acetate) as mobile phase, and UV lamp (254 nm) were employed to spots detection. Purification of compounds were carried out on a CombiFlash®RF instrument (Teledyne Isco) employing Silica RediSep Rf gold® columns in a normal phase gradient. For the chemical characterization an Infrared spectra (IR), proton nuclear magnetic resonance ($^1$H NMR), carbon nuclear magnetic resonance ($^{13}$C NMR) and elemental microanalyses (CHN) were employed. IR spectrums were analysed on a Nicolet Nexus FTIR (Thermo Madison) employing KBr pellets. Absorption values are given in $cm^{-1}$ and reported only significant absorption bands as medium (m) and strong (s). 400 MHz $^1$H and 100 MHz $^{13}$C NMR spectroscopy were carried out on a Bruker 400 Ultrashield using TMS as an internal reference. Chemical shifts (δ), expressed in ppm, were referenced according to DMSO-$d_6$ or $CDCl_3$ solvents.[78] Coupling constants (*J*) were given in hertz (Hz) and multiplicities detected in $^1$H NMR were reported as singlet (s), bs (broad singlet), doublet (d), doublet of doublets (dd), triplet (t) and multiplet (m). In some cases, 2D NMR were performed for assigning peaks (HMBC and HMQC). Purity of final compounds

ACCEPTED MANUSCRIPT

was ≥95% and it was carried out on a CHN-900 elemental analyzer (Leco, TresCantos). Elemental analysis of C, H, and N values were within the range of ± 0.4 with respect to theoretical values. Melting points were conducted using a Mettler FP82 + FP80 (Greifensee) and were uncorrected.

*4.1.2. Synthesis of the intermediate compound*

*4.1.2.1. Synthesis of 1-(4-methoxyphenyl)prop-2-en-1-one (**i1**).* **i1** was synthesized according to Bugarin *et al* with some modifications [44]. Briefly, a mixture of 4′-methoxyacetophenone (1.0 mmol), paraformaldehyde (8.0 equiv.), and diisopropylammonium 2,2,2-trifluoroacetate (1.0 equiv.) were dissolved in THF (10 mL), then, trifluoroacetic acid (0.1 equiv.) was added. The mixture reaction was stirred under reflux for 8 h. After that, THF was removed and the residue was diluted in diethyl ether. The organic phase was washed with HCl 1M, NaOH 1M and brine (saturated NaCl solution), dried over anhydrous $Na_2SO_4$, filtered, and evaporated.

*4.1.3. Synthesis and Chemical characterization of Mannich bases-type derivatives (**1-10**)*

The general procedure for the synthesis of compounds **1-6** was following Michael reaction between vinyl ketones and arylamines. A mixture of **i1** (3.0 mmol) and the corresponding amine (3.0 mmol) was diluted in $CH_2Cl_2$ (20 mL). The reaction was stirred at room temperature and the reaction completion was determined by TLC (24 to 48 h). The crude was purified by automated flash chromatography with $CH_2Cl_2$/methanol solvent system as the eluent (in gradient). The final compound was precipitated with cold diethyl ether.

On the other hand, the synthesis of compounds **7-10** was performed by Mannich reaction following the procedures previously reported with some modifications.[41, 45] A mixture of 4′-hydroxyacetophenone (2.0 mmol), the corresponding aryl-piperazine (2.0 mmol), 1,3-dioxolane (5 mL) and concentrated HCl (0.5 mL) was refluxed until TLC proved that the reaction did not go (20 to 40 min). Products were obtained by vacuum filtration and they were purified either by automated flash chromatography, eluting in gradient with $CH_2Cl_2$/methanol, and finally washed with acetone or only washing with acetone.

*4.1.3.1. 1-(4-Methoxyphenyl)-3-((4-(trifluoromethyl)phenyl)amino)propan-1-one (**1**).* Yield: 20%. Mp: 154-155 ºC. IR (KBr) ν $cm^{-1}$: 3399 (s, $\nu_{N-H}$); 1665 (s, $\nu_{C=O}$); 1170 (s, $\nu_{C-F}$); 1110 (s, $\nu_{C-F}$); 1069 (s, $\nu_{C-F}$). $^1$H NMR (DMSO-$d_6$, 400 MHz) δ ppm: 7.96 (d, 2H, **H$_2$** + **H$_6$**, $J_{2-3}$ = 8.8 Hz); 7.37 (d, 2H, **H$_{3'}$** + **H$_{5'}$**, $J_{3'-2'}$ = 8.6 Hz); 7.04 (d, 2H, **H$_3$** + **H$_5$**, $J_{3-2}$ = 8.8 Hz); 6.69 (d, 2H, **H$_{2'}$** + **H$_{6'}$**, $J_{2'-3'}$ = 8.6 Hz); 3.84 (s, 3H, **OCH$_3$**); 3.43 (t, 2H, **CH$_2$**, $J_{CH2-CH2}$ = 6.5 Hz); 3.26 (t, 2H,

ACCEPTED MANUSCRIPT

**CH₂**, $J_{CH2\text{-}CH2}$ = 6.5 Hz). $^{13}$C NMR (APT, DMSO-$d_6$, 100MHz) δ ppm: 197.29; 163.64; 152.05; 130.69 (2C); 130.10; 126.70 (2C, q, $^3J$= 3.7 Hz); 125.87 (q, $^1J$= 269.7 Hz); 115.61 (q, $^2J$ = 31.9 Hz); 114.35 (2C); 111.71 (2C); 55.98; 38.14; 37.40. Anal. Calc. for $C_{17}H_{16}F_3NO_2$: C 63.15%, H 4.99%, N 4.33%. Found: C 63.45%, H 5.01%, N 4.55%.

*4.1.3.2. 3-((4-Fluorophenyl)amino)-1-(4-methoxyphenyl)propan-1-one (**2**).* Yield: 36%. Mp: 144-145 ºC. IR (KBr) ν cm$^{-1}$: 3371 (s, $\nu_{N\text{-}H}$); 1665 (s, $\nu_{C=O}$). $^1$H NMR (DMSO-$d_6$, 400 MHz) δ ppm: 7.94 (d, 2H, **H₂** + **H₆**, $J_{2\text{-}3}$ = 8.9 Hz); 7.04 (d, 2H, **H₃** + **H₅**, $J_{3\text{-}2}$ = 8.9 Hz); 6.91 (d, 2H, **H₃'** + **H₅'**, $J_{3'\text{-}2'}$ = 8.9 Hz); 6.57 (dd, 2H, **H₂'** + **H₆'**, $J_{2'\text{-}3'}$ = 9.0 Hz, $J_{2'\text{-}F}$ = 4.6 Hz); 5.49 (t, 1H, **NH**, $J_{NH\text{-}CH2}$ = 5.7 Hz); 3.84 (s, 3H, **OCH₃**); 3.37-3.30 (m, 2H, **CH₂ + H₂O**); 3.21 (t, 2H, **CH₂**, $J_{CH2\text{-}CH2}$ = 6.5 Hz). $^{13}$C NMR (APT, DMSO-$d_6$, 100MHz) δ ppm: 197.63; 163.60; 154.75 (d, $^1J$ = 230.9 Hz); 145.88, 130.68 (2C); 130.17; 115.72 (2C, d, $^2J$ = 21.9 Hz); 114.35 (2C); 113.24 (2C, d, $^3J$ = 7.3 Hz); 55.98; 39.30; 37.70. Anal. Calc. for $C_{16}H_{16}FNO_2$: C 70.31%, H 5.90%, N 5.12%. Found: C 70.34%, H 5.50%, N 5.02%.

*4.1.3.3. 3-((4-Chlorophenyl)amino)-1-(4-methoxyphenyl)propan-1-one (**3**).* Yield: 26%. Mp: 154-155 ºC. IR (KBr) ν cm$^{-1}$: 3369 (s, $\nu_{N\text{-}H}$); 1665 (s, $\nu_{C=O}$). $^1$H NMR (DMSO-$d_6$, 400 MHz) δ ppm: 7.94 (d, 2H, **H₃ + H₅**, $J_{3\text{-}2}$ = 8.8 Hz); 7.13-6.99 (m, 4H, **H₂ + H₆ + H₃' + H₅'**); 6.59 (d, 2H, **H₂' + H₆'**, $J_{2'\text{-}3'}$ = 8.8 Hz); 5.80 (t, 1H, **NH**, $J_{NH\text{-}CH2}$ = 5.5 Hz); 3.84 (s, 3H, **OCH₃**); 3.41-3.30 (m, 2H, **CH₂ + H₂O**); 3.23 (t, 2H, **CH₂**, $J_{CH2\text{-}CH2}$ = 6.5 Hz). $^{13}$C NMR (APT, DMSO-$d_6$, 100MHz) δ ppm: 197.50; 163.61; 148.06; 130.69 (2C); 130.14; 129.06 (2C); 119.32; 114.36 (2C); 113.79 (2C); 56.00; 38.71; 37.56. Anal. Calc. for $C_{16}H_{16}ClNO_2$: C 66.32%, H 5.57%, N 4.83%. Found: C 66.47%, H 5.39%, N 4.90%.

*4.1.3.4. 1-(4-Methoxyphenyl)-3-((4-(trifluoromethyl)phenethyl)amino)propan-1-one (**4**).* Yield: 19%. mp: 88-89 ºC. IR (KBr) ν cm$^{-1}$: 3297 (m, $\nu_{N\text{-}H}$); 1667 (s, $\nu_{C=O}$); 1170 (m, $\nu_{C\text{-}F}$); 1120 (m, $\nu_{C\text{-}F}$); 1069 (s, $\nu_{C\text{-}F}$). $^1$H NMR ($CDCl_3$, 400 MHz) δ ppm: 7.86 (d, 2H, **H₃** + **H₅**, $J_{3\text{-}2}$ = 8,9 Hz); 7.47 (d, 2H, **H₃'** + **H₅'**, $J^{3'\text{-}2'}$ = 8.1 Hz); 7.25 (d, 2H, **H₂** + **H₆**, $J_{2\text{-}3}$ = 8.0 Hz); 6.86 (d, 2H, **H₂'** + **H₆'**, $J_{2'\text{-}3'}$ = 6.9 Hz); 3.80 (s, 3H, **OCH₃**); 3.06 (t, 2H, **CH₂**, $J_{CH2\text{-}CH2}$ = 6.3 Hz); 2.96 (t, 2H, **CH₂**, $J_{CH2\text{-}CH2}$ = 6.1 Hz); 2.89-2.83 (m, 2H, **CH₂**); 6.79 (t, 2H, **CH₂**, $J_{CH2\text{-}CH2}$ = 6.8 Hz). $^{13}$C NMR (APT, $CDCl_3$, 100 MHz) δ ppm: 198.02; 163.60; 144.26; 130.29 (2C); 129.99; 129.00 (2C); 128.47 (q, $^2J$ = 32.6 Hz); 125.34 (2C, q, $^3J$ = 3.7 Hz); 124.33 (q, $^1J$ = 271.4 Hz); 113.76 (2C); 55.45; 51.00; 44.69; 38.27; 36.29. Anal. Calc. for $C_{19}H_{20}F_3NO_2$: C 64.95%, H 5.74%, N 3.99%. Found: C 64.94%, H 5.65%, N 3.91%.

ACCEPTED MANUSCRIPT

*4.1.3.5. 3-((4-Fluorophenethyl)amino)-1-(4-methoxyphenyl)propan-1-one (**5**).* Yield: 25%. Mp: 75-76 ºC. IR (KBr) ν $cm^{-1}$: 3297 (m, $\nu_{N-H}$); 1671 (s, $\nu_{C=O}$); 1216 (s, $\nu_{C-F}$). $^1$H NMR ($CDCl_3$, 400 MHz) δ ppm: 8.17-7.86 (m, 2H, **H₃ + H₅**); 7.42-6.85 (m, 6H, **H₂ + H₆ + H₂' + H₃' + H₅' + H₆'**); 3.87 (s, 3H, **OCH₃**); 3.25-2.68 (m, 8H, **CH₂**). $^{13}$C NMR (APT, $CDCl_3$, 100 MHz) δ ppm: 197.97; 163.50; 161.40 (d, $^1J$ = 239.9 Hz); 135.61; 130.27; 130.22 (2C); 129.96 (2C, d, $^3J$ = 7.8 Hz); 115.12 (2C, d, $^2J$ = 21.1 Hz); 113.68 (2C); 55.38; 51.40; 44.66; 38.28; 35.56. Anal. Calc. for $C_{18}H_{20}FNO_2$: C 71.74%, H 6.69%, N 4.65%. Found: C 71.34%, H 6.41%, N 4.63%.

*4.1.3.6. 3-((4-Chlorophenethyl)amino)-1-(4-methoxyphenyl)propan-1-one (**6**).* Yield: 20%. Mp: 98-99 ºC. IR (KBr) ν $cm^{-1}$: 3297 (m, $\nu_{NH}$); 1671 (s, $\nu_{C=O}$). $^1$H NMR ($CDCl_3$, 400 MHz) δ ppm: 7.85 (d, 2H, **H₃ + H₅**, $J_{3-2}$ = 8,9 Hz); 7.18 (d, 2H, **H₃' + H₅'**, $J_{3'-2'}$ = 8.4 Hz); 7.06 (d, 2H, **H₂' + H₆'**, $J_{2'-3'}$ = 8.4 Hz); 6.86 (d, 2H, **H₂ + H₆**, $J_{2-3}$ = 8.9 Hz); 3.80 (s, 3H, **OCH₃**); 3.05 (t, 2H, **CH₂**, $J_{CH2-CH2}$ = 6.1 Hz); 2.95 (d, 2H, **CH₂**, $J_{CH2-CH2}$ = 6.2 Hz); 2.82 (t, 2H, **CH₂**, $J_{CH2-CH2}$ = 7.1 Hz); 2.70 (t, 2H, **CH₂**, $J_{CH2-CH2}$ = 7.2 Hz). $^{13}$C NMR (APT, $CDCl_3$, 100 MHz) δ ppm: 197.93; 163.48; 138.44; 131.77; 130.20 (2C); 129.95 (2C); 128.45 (2C); 128.21; 113.67 (2C); 55.37; 51.14; 44.63; 38.24; 35.71. Anal. Calc. for $C_{18}H_{20}ClNO_2$: C 68.03%, H 6.34%, N 4.41%. Found: C 68.41%, H 6.30%, N 4.36%.

*4.1.3.7. 1-(4-Hydroxyphenyl)-3-(4-(4-(trifluoromethyl)phenyl)piperazin-1-yl)propan-1-one hydrochloride (**7**).* Yield: 56%. Mp: 189-190 ºC. IR (KBr) ν $cm^{-1}$: 1678 (s, $\nu_{C=O}$); 1170 (s, $\nu_{C-F}$); 1104 (s, $\nu_{C-F}$); 1072 (s, $\nu_{C-F}$). $^1$H NMR (DMSO-$d_6$, 400 MHz) δ ppm: 11.44-11.27 (bs, 1H, **HCl**); 10.62 (s, 1H, **OH**); 7.90 (d, 2H, **H₂ + H₆**, $J_{2-3}$ = 8.8 Hz); 7.56 (d, 2H, **H₃' + H₅'**, $J_{3'-2'}$ = 8.8 Hz); 7.16 (d, 2H, **H₂' + H₆'**, $J_{2'-3'}$ = 8.8 Hz); 6.92 (d, 2H, **H₃ + H₅**, $J_{3-2}$ = 8.8 Hz); 4.10-3.97 (m, 2H, **CH₂**); 3.73-3.57 (m, 4H, **Hp**); 3.52-3.42 (m, 2H, **CH₂**); 3.35-3.11 (m, 4H, **Hp**). $^{13}$C NMR (APT, DMSO-$d_6$, 100 MHz) δ ppm: 194.56, 162.56, 151.93, 130.51 (2C), 127.39, 126.22 (2C, q, $^3J$ = 3.2 Hz), 124.72 (q, $^1J$ = 270.7 Hz), 118.84 (q, $^2J$ = 31.9 Hz), 115.26 (2C), 114.84 (2C), 50.84, 50.40 (2C), 44.20 (2C), 32.07. Anal. Calc. for $C_{20}H_{21}F_3N_2O_2$.HCl: C 57.90%, H 5.35%, N 6.75%. Found: C 58.26%, H 5.49%, N 7.00%.

*4.1.3.8. 3-(4-(4-Fluorophenyl)piperazin-1-yl)-1-(4-hydroxyphenyl)propan-1-one hydrochloride (**8**).* Yield: 20%. Mp: 191-192 ºC. IR (KBr) ν $cm^{-1}$: 1675 (s, $\nu_{C=O}$); 1170 (s, $\nu_{C-F}$). $^1$H NMR (DMSO-$d_6$, 400 MHz) δ ppm: 11.23-11.00 (bs, 1H, **HCl**); 10.59 (s, 1H, **OH**); 7.90 (d, 2H, **H₂ + H₆**, $J_{2-3}$ = 8.4 Hz); 7.14-6.98 (m, 4H, **H₂' + H₃' + H₅' + H₆'**); 6.91 (d, 2H, **H₃ + H₅**, $J_{3-5}$ = 8.4 Hz); 3.79-3.69 (m, 2H, **CH₂**); 3.69-3.56 (m, 4H, **Hp**); 3.52-3.41 (m, 2H, **CH₂**); 3.28-3.05 (m, 4H, **Hp**). $^{13}$C NMR (APT, DMSO-$d_6$, 100 MHz) δ ppm: 194.59, 162.53, 156.51 (d, $^1J$

ACCEPTED MANUSCRIPT

= 236.8 Hz), 146.39, 130.53 (2C), 127.41, 117.79 (2C, d, $^{3}J$ = 7.6 Hz), 115.41 (2C, d, $^{2}J$ = 22.2 Hz), 115.26 (2C), 50.82 (3C), 46.10 (2C), 32.10. Anal. Calc. for $C_{19}H_{21}FN_2O_2$.HCl: C 62.55%, H 6.08%, N 7.68%. Found: C 62.85%, H 6.12%, N 7.86%.

*4.1.3.9. 3-(4-(4-Chlorophenyl)piperazin-1-yl)-1-(4-hydroxyphenyl)propan-1-one hydrochloride (**9**).* Yield: 26%. Mp: 194-195 ºC. IR (KBr) ν $cm^{-1}$: 1674 (s, $\nu_{C=O}$). $^{1}$H NMR (DMSO-$d_6$, 400 MHz) δ ppm: 11.37-11.02 (bs, 1H, **HCl**); 10.62 (s, 1H, **OH**); 7.90 (d, 2H, **H₂ + H₆**, $J_{2-3}$ = 8.7 Hz); 7.28 (d, 2H, **H₃' + H₅'**, $J_{3'-2'}$ = 8.9 Hz); 7.03 (d, 2H, **H₂' + H₆'**, $J_{2'-3'}$ = 8.9 Hz); 6.91 (d, 2H, **H₃ + H₅**, $J_{3-2}$ = 8.7 Hz); 3.92-3.74 (m, 2H, **CH₂**); 3.71-3.53 (m, 4H, **Hp**); 3.52-3.40 (m, 2H, **CH₂**); 3.35-3.11 (m, 4H, **Hp**). $^{13}$C NMR (APT, DMSO-$d_6$, 100 MHz) δ ppm: 194.64, 162.55, 148.41, 130.54 (2C), 128.73 (2C), 127.42, 123.45, 117.43 (2C), 115.28 (2C), 50.84, 50.63 (2C), 45.24 (2C), 32.14. Anal. Calc. for $C_{19}H_{21}ClN_2O_2$.HCl: C 59.85%, H 5.82%, N 7.35%. Found: C 59.47%, H 6.00%, N 6.97%.

*4.1.3.10. 1-(4-Hydroxyphenyl)-3-(4-(4-nitrophenyl)piperazin-1-yl)propan-1-one hydrochloride (**10**).* Yield: 22%. Mp: 196-197 ºC. IR (KBr) ν $cm^{-1}$: 1677 (s, $\nu_{C=O}$); 1597 (s, $\nu_{NO2}$); 1318 (s, $\nu_{NO2}$). $^{1}$H NMR (DMSO-$d_6$, 400 MHz) δ ppm: 11.65-11.44 (bs, 1H, **HCl**); 10.64 (s, 1H, **OH**); 8.10 (d, 2H, **H₃' + H₅'**, $J_{3'-2'}$ = 9.4 Hz); 7.89 (d, 2H, **H₂ + H₆**, $J_{2-3}$ = 8.7 Hz); 7.14 (d, 2H, **H₂' + H₆'**, $J_{2'-3'}$ = 9.4 Hz); 6.91 (d, 2H, **H₃ + H₅**, $J_{3-2}$ = 8.7 Hz); 4.32-4.07 (m, 2H, **CH₂**); 3.76-3.39 (m, 8H, **Hp + CH₂**); 3.25-3.11 (m, 2H, **Hp**). $^{13}$C NMR (APT, DMSO-$d_6$, 100 MHz) δ ppm: 194.66, 162.57, 153.76, 137.89, 130.53 (2C), 127.41, 125.56 (2C), 115.28 (2C), 113.43 (2C), 50.89, 50.34 (2C), 43.63 (2C), 32.17. Anal. Calc. for $C_{19}H_{21}FN_3O_4$.HCl: C 58.24%, H 5.66%, N 10.72%. Found: C 57.85%, H 6.02%, N 10.51%.

*4.2. In vitro biological assays*

*4.2.1. Mammalian Cell culture and cytotoxicity assay on Vero cells*

Vero Cells from african green monkey kidney (EACC number 84113001), were grown in RPMI-1640 medium (Gibco®) supplemented with 10% heat inactivated foetal bovine serum (FBS, Gibco®), antibiotics, at 37 ºC and 5% $CO_2$. Stock solutions of studied compounds (synthesized Mannich base derivatives and BZN) were dissolved in 100% DMSO. So, compounds were tested for cytotoxicity evaluation against Vero Cells to determine the $IC_{50}$ as previously described by Garnica *et al.*[79] Briefly, cells during the logarithmic growth phase were seeded in 96-well plates ($0.8 \times 10^4$ cell/well) to be exposed to serial dilutions of compounds (from 10.0 to 200.0 µM). After 72 h MTT (*3-(4,5-dimethylthiazol-2-yl)-2,5-*

ACCEPTED MANUSCRIPT

*diphenyltetrazolium bromide*) was added and after a further 4 h, absorbances measurements were determined using a Tecan Sunrise™ Microplate Reader. Each studied concentration was assayed in quadruplicate in three independent experiments. $IC_{50}$ values were calculated through nonlinear regression (log(inhibitor) *vs.* normalized response-variable slope) equation employing GraphPad Prism 7 software.

*4.2.2. Parasites and compounds*

The studied compounds were tested against three different strains of *T. cruzi*, including SN3 strain (IRHOD/CO/2008/SN3; DTU I), obtained from domestic *Rhodnius prolixus* (Guajira, Colombia)[80]; Arequipa strain (MHOM/Pe/2011/Arequipa; DTU V), isolated from a human (Arequipa, Peru) and Tulahuen strain (TINF/CH/1956/Tulahuen; DTU VI) isolated from Tulahuen, Chile. Furthermore, they were evaluated against three different morphological forms of the parasite (epimastigote, trypomastigote and amastigote forms).

Compounds and BZN were dissolved in 100% DMSO to prepare stock solutions. Further work dilutions were prepared on culture medium before the experiment.

*4.2.3. Extracellular epimastigote forms assessment*

Epimastigotes forms of *T. cruzi* were grown in medium trypanosomes liquid (MTL) supplemented with 10% heat inactivated FBS at 28 ºC.[60] Compounds were tested for *in vitro* antiparasitic activity on epimastigote forms as procedure described.[81] Compounds, at five levels of concentration (from 6.3 μM to 50 μM), were added to suspensions of $5 \times 10^5$ parasites/ml in 96-well plates at 28ºC. After 48 h, resazurin sodium salt (Sigma-Aldrich) was added and incubated for further 24 h. After this period the absorbances were measured employing a microplate reader (Sunrise™, TECAN) at 570 and 600 nm.[82] The $IC_{50}$ were then generated for each dose-response curve (nonlinear regression; log(inhibitor) vs. normalized response-variable slope) using GraphPad Prism 7 software. Each level of concentration was carried out in triplicate, and the experiments were performed three times.

*4.2.4. Transformation of epimastigotes to metacyclic forms*

Metacyclogenesis from epimastigotes into metacyclic forms, to infect BALC/c albino mice, was tested according to Cardoso and Soares.[83]

*4.2.5. Bloodstream trypomastigotes assessment*

Blood containing the trypomastigote forms were extracted via cardiac puncture from BALB/c albino mice and diluted in RPMI (Gibco®) supplemented with 10% heat-inactivated FBS

ACCEPTED MANUSCRIPT

(Gibco®) according to previous publications.[81] Compounds **2-4**, **7**, **9** and BZN were evaluated against this parasite forms. The protocol was done as procedure previously described by Moreno-Viguri *et al*, with certain modifications.[84-85] Studied compounds and reference drug were diluted to obtain different concentrations ranging from 3.1 to 50.0 μM, although, in some compounds it was necessary to test lower doses to determine the $IC_{50}$. By triplicate in at least three separate experiments, parasites at $2 \times 10^6$ trypomastigotes/mL were seeded in culture plates of 96-well and the compounds were added to be incubated for 24 h at 37 ºC in 5% $CO_2$. After this period, the trypomastigotes number were counted microscopically employing a Neubauer chamber. Results were determined by nonlinear regression (log(inhibitor) vs. normalized response-variable slope) equation using Graphpad Prism 7 software.

*4.2.6. Intracellular amastigote forms and infected Vero cells assessment*

This *in vitro* activity was conducted as described previously in the literature.[85-86] Vero cells were maintained in supplemented RPMI (Gibco ®) as described above (see *Mammalian Cell culture and cytotoxicity assay on Vero cells section)*. During the exponential grown phase, $1 \times 10^4$ Vero cells/well were distributed in 24-well cultured plates (each well contains a circular coverslip) and incubated at 37 °C and 5% $CO_2$ during 24 h. Afterwards, trypomastigotes were added to infect the adhered Vero cells (multiplicity of infection ratio, 10:1). After 24 h, extracellular parasites were removed by three successive washes with PBS and compounds **2-4**, **7** and **9** and BZN at different concentrations (3.1, 6.25, 12.5, 25 and 50 μM) were added. After 72 h of incubation at the same conditions, the number of amastigote forms and infected Vero cells were determined via Giemsa staining. Each studied concentration was made in triplicate and the experiments were made in two separate determinations. The $IC_{50}$ were calculated using Graphpad Prism 7 software by nonlinear regression (log(inhibitor) vs. normalized response-variable slope) equation.

*4.2.7. In vitro Genotoxicity assessment*

*4.2.7.1. SOS/UMU-test*

This screening was carried out to determine the genotoxic potential of selected compounds and some of their metabolites using a *Salmonella typhimurium* TA1535/pSK1002 test strain (DSMZ, Germany) in 96 well-plates with and without S9 metabolic activation as described Perez-Silanes *et al.*[87] Firstly, the bacterial survival percentage was measured by exposing this

ACCEPTED MANUSCRIPT

bacterial strain against the selected compounds at different concentrations in the presence or absence of S9 mix (Mutazyme$^{TM}$). Later, the β-galactosidase activity was evaluated by a colorimetric method, employing an o-nitrophenyl-β-D-galactopyranoside (ONPG) as substrate. Also, assay controls were considered in the experiment. Finally, the genotoxic activity was expressed in terms of enzymatic units (relative units, RU) and in enzyme induction factor (induction factor, IF). This experiment is considered acceptable if the IF ≥ 2 for positive controls. So, a compound was considered genotoxic if the IF ≥ 2 at non-cytotoxic concentration (which means that the bacteria survival percentage is ≥80%).

*4.2.8. In vivo trypanocidal activity assessment*

*4.2.8.1. Mice and infection*

The study was approved by the ethics committee on animal experimentation of University of Granada, Spain (RD53/2013), following the international guiding principles for biomedical research involving experimental animals. Group of three female BALB/c mice of 10-12 weeks old, weighing 14-20 g were used in these experiments. Animals were kept in clean ventilated cages and maintained on a 12/12 (light/dark) h cycle and a temperature of 22 ± 3 ºC with access to ad libitum standard food and water.

BALB/c mice were injected intraperitoneally (i.p.) with $5 \times 10^5$ bloodstream trypomastigotes in 0.2 mL PBS, freshly obtained from mice previously infected with metacyclic trypomastigotes of Arequipa *T. cruzi* strain. On the seventh day post-infection (pi) the parasitemia in peripheral blood was confirmed.

*4.2.8.2. Treatment*

BZN and testing compounds were prepared at 2 mg/ml in an aqueous suspension vehicle containing DMSO (5%) and hydroxypropyl methylcellulose (0.5%) as described in the literature.[62]

Animals were randomly divided in acute and chronic phase in the following groups: Negative control group (uninfected and non-treated mice); positive control group (infected and non-treated mice); BZN group (infected mice treated with BZN); and study group (infected mice treated with studied compounds). In acute and chronic phase, the different groups began to receive the respective treatment on day 8 pi and day 70 pi, respectively. BZN and compounds were dosed orally at 20 mg/kg/day (0.2 mL) during five consecutive days and control groups received only vehicle. Experiments were conducted in groups of three mice.

ACCEPTED MANUSCRIPT

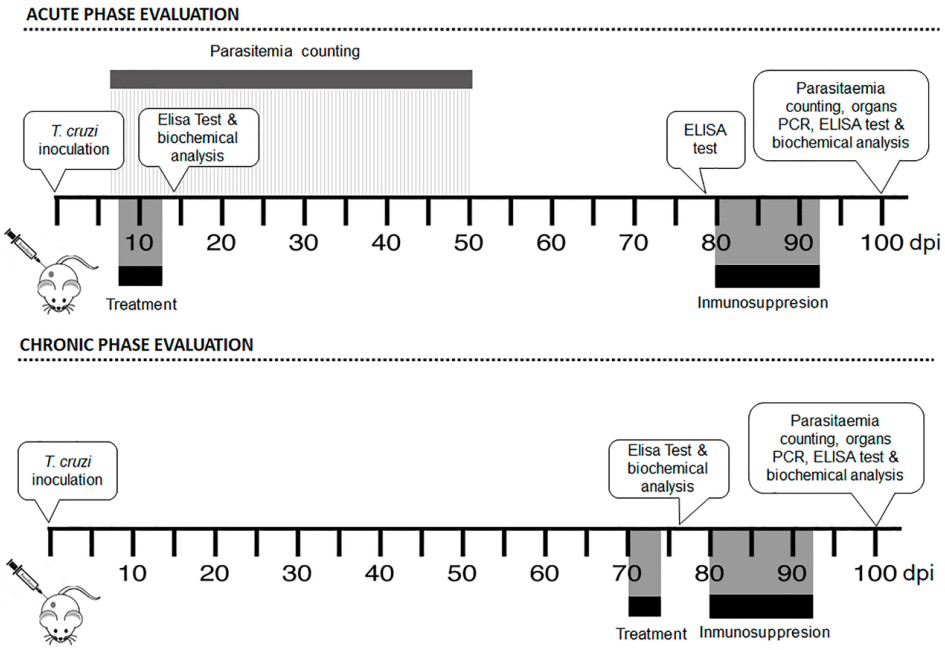


**Scheme 2.** Outline of *in vivo* experiments in both acute and chronic phases of Chagas disease.

*4.2.8.3. Parasitemia levels during the acute phase treatment*

Parasitemia levels were obtained from the count of bloodstream trypomastigotes in the peripheral blood dissolved in PBS (1:100 / blood:PBS) using the Neubauer chamber.[88] This determination is made every 2 to 3 days, from day 7 pi until no parasitemia levels are undetectable.

*4.2.8.4. Ciclophosphamide administration*

Once the BALB/c mice were treated in acute and chronic phase and also in both groups no blood parasitemia was detected (day 80 pi), cyclophosphamide (CP, ISOPAC®) was administered intraperitoneally at the doses of 200 mg / kg for their immunosuppression according to specified by Francisco *et al.*[28] After CP administration, parasitemia levels are determined based on the count of the bloodstream parasitic forms to calculate the reactivation rate.[40]

*4.2.8.5. Blood and organs extraction*

After evaluating the reactivation through immunosuppression, mice were sacrificed by exsanguination (cardiac puncture) under $CO_2$ gas exposure. Blood was collected and treated to obtain the serum to Elisa and biochemical studies.[60] Also, some organs and tissues (adipose, bone marrow, brain, oesophagus, heart, lung, muscle, spleen, and stomach) were excised and

ACCEPTED MANUSCRIPT

spleens were weighed to assess their possible inflammation. Then, organs and tissues were perfused with pre-warmed PBS and stored until DNA extraction according to the literature.[84]

*4.2.8.6. DNA extraction and PCR analyses*

The removed organs were ground, and the DNA was extracted using a Wizard® Genomic DNA Purification Kit (Promega). PCR was carried out based on the sequence of the *T. cruzi* splice leader (SL) intergenic region using two published primers (TC and TC1) that allow the amplification of a 300 base pairs fragment in different biological samples. The amplifications were performed using a Thermal Cycler TM MyCycler thermal cycler (Bio-Rad) using the commercial BioMix™ (Bioline), adding 200 nM of each primer and 5 % DMSO (final volume of 20 μL), with the following routine: 94 °C/4 min, 27 cycles of 94 °C/30 s, 55 °C/30 s, 72 °C/30 s, and 72 °C/5 min. Finally, the PCR products were resolved according to the literature.[40]

*4.2.8.7. Indirect ELISA test*

This assay was performed to determine the changes of antibody levels in different stages of the study, both acute and chronic phase. The samples (serum) were obtained in acute phase: two days after the treatment, one day before the immunosuppression and the day of the necropsy; in chronic phase: two days after the treatment and the day of the necropsy **(Scheme 2)**. The assay was performed as described by Olmo *et al.*[89] Fe-SOD, obtained according to López-Cespedes *et al*, [59] was used as an antigen fraction. The measurements were made in a microplate reader (Sunrise™, TECAN) at 492 nm.

*4.2.8.8. Toxicity tests by biochemical analysis*

The blood samples were collected, both acute and chronic phase, two days after the treatment and in the day of necropsy **(Scheme 2)**. Serum levels of alkaline phosphatase (ALP), aspartate aminotransferase (AST/GOT), alanine aminotransferase (ALT/GPT), creatine kinase-muscle/brain (CK-MB), lactate dehydrogenase (LDH), total bilirubin, urea and uric acid were measured by commercial kits (Cromakit®) using BS-20 Chemistry analyser Shenzhen Mindray (Bio-medical Electronics Co. LDT) in the Biochemical Service of the University of Granada.

*4.2.9. Mechanism of action studies.*

*4.2.9.1. Metabolite excretion*

This study was performed according to the procedure already published with certain modifications.[90] Briefly, epimastigote forms of Arequipa *T. cruzi* strain in logarithmic growth

ACCEPTED MANUSCRIPT

phase, grown in supplemented MTL at 28 ºC,[60] were centrifugated (400 × g for 10 min) and diluted back in culture flasks at $5 \times 10^5$ parasites/mL. Then, the $IC_{50}$ of the compounds and BZN (except for non-treated cultures) were added to the flasks. After 72 h at 28 ºC, epimastigote forms were centrifuged (800 × g for 10 min) and the supernatant were collected for the $^1$H NMR analysis. The $^1$H NMR was done in a Varian direct drive 400 MHz spectrometer using TMS as the reference signal. The Mestrecnova 9.0. software was employed to identify the excreted metabolites according to Fernandez Becerra *et al.*[91]

*4.2.9.2. Rhodamine 123 (Rho) and acridine orange (AO) assays*

For this assay, cultures of epimastigote forms of Arequipa *T. cruzi* strain ($5 \times 10^5$ parasites/mL) were exposed to the $IC_{50}$ of compounds and BZN. After 72 h of incubation at 28 °C, samples were treated with rhodamine 123 (Rho 123) or acridine orange (AO) and measured by flow cytometry according to the procedure described in the literature.[40] The changes in the fluorescence intensities were expressed in the index of variation (IV), that were calculated as follow: IV = (TM–CM)/CM, where TM is the median fluorescence for treated epimastigote forms and CM is that for non-treated epimastigote forms.[92]

*4.2.9.3. Extraction the SOD excreted and in vitro SOD inhibition evaluation*

Cultures of *T. cruzi* epimastigote forms (Arequipa strain) were grown in supplemented MTL at 28 ºC.[59] Parasites in exponential growth and the protein excreted were treated according to Martin-Escolano *et al.*[40] Protein was quantified via Bradford method.[93] CuZn-SOD (Sigma Aldrich) and Fe-SOD excreted activities were calculated following the protocol described by Beyer and Fridovich.[94]

*4.2.10. Mutagenicity assay*

*4.2.10.1. Ames test*

The evaluation of the mutagenic capacity of the selected compound was performed using a miniaturized version of the Ames test, in which 6 well plates are used instead of Petri dishes. The assay was performed following the principles of the plate incorporation method included in the OECD guideline for the Ames test.[72] Compound **9** was tested on 5 strains of *Salmonella typhimurium:* TA97a, TA 98, TA 100, TA 102, and TA 1535 (Trinova, Biochem GmbH); in absence or presence of an external enzymatic metabolizing system (S9 mix, Mutazyme™, Moltox).

ACCEPTED MANUSCRIPT

Firstly, a solubility test was performed in order to elucidate the highest concentration to test. Bacteria were exposed to different concentrations of the test compound. Briefly, a mixture of each concentration of compound (20 µL), bacterial suspension (25 µL), soft agar supplemented with histidine/biotine (500 µL) and S9 mix or PBS (100 µL), was prepared in Eppendorf tube placed on a termoblock at 47 ºC under soft agitation. The mixture was poured onto pre-warmed glucose minimal agar in 6 well/plates. After 1h drying at room temperature (plates face up), all the plates were incubated for 48 h at 37 ºC in an incubator (plates upside down). Negative and positive controls were included in the experiment. Regarding positive controls, the following compounds were used: nitro-o-phenylendiamine for the strains TA97a, TA98 and TA100, mitomycin C for the strain TA102, sodium azide for the strain TA1535, 2-aminoantracene with external metabolic activation for the strains TA97a and TA1535, and 2-aminofluorene with external metabolic activation for the strains TA98, TA 100 and TA102. Three technical triplicates were used per conditions (i.e., 3 wells). After the incubation, colonies were counted using the colony counter Celeromics (Celeromics Technology). Results were expressed as mean and standard deviation from the technical triplicates (**Table 6**).

*4.3. Docking study*

The compounds protonation state at pH 7.4 was estimated by the chemicalize web server (http://www.chemicalize.org/), and afterwards they were designed with the program Avogadro.[95] AM1 charges were calculated with the Chimera software.[77] As target for the docking, the structure with PDB entry 4DVH, of the mitochondrial *T. cruzi* Fe-SOD protein, was used, with the residue numbering according to that of Martinez *et.al*, i.e., without the mitochondrial signal peptide.[96] The protein protonation state at pH 7.4 was obtained with the program PDB2PQR,[97] and Gasteiger charges for the protein were added with Autodock.[98] The docking study was performed with the Autodock4.0 program, using the Lamarckian genetic algorithm (LGA),[99] with a grid centered on the dimer interface, as defined in a previous article by our group.[41]

**Acknowledgments**

The research leading to these results has received funding from Obra Social la CAIXA (LCF/PR/PR13/11080005) and Fundación Caja Navarra, Fundación María Francisca de Roviralta and, Ubesol. Former Spanish Ministry of Science and Innovation (MICINN), the Ministry of Economy and Competitiveness (MINECO) (project Consolider Ingenio CSD2010-

ACCEPTED MANUSCRIPT

00065). R.M-E. is grateful for a FPU Grant (FPU14/01537) from the Ministry of Education of Spain. R.P. is indebted to the Asociación de Amigos de la Universidad de Navarra for a grant. A.A. thanks the Ministry of Economy, Industry and Competitiveness ('Ramón y Cajal' programme, RYC2013-14370) of the Spanish Government for personal support.

## Appendix A. Supplementary data

Supplementary data related to this article can be found online at.

## REFERENCES

1. DND*i*. About Chagas disease. https://www.dndi.org/diseases-projects/chagas/; 2018. Accessed 13 March 2019.
2. WHO. Investing to overcome the global impact of neglected tropical diseases: third WHO report on neglected tropical diseases, Chagas disease. https://www.who.int/neglected_diseases/9789241564861/en/; 2015. Accessed 27 November 2018.
3. WHO. Chagas disease in Latin America: an epidemiological update based on 2010 estimates. *Wkly. Epidemiol. Rec.* 2015;90:33-44.
4. Lee BY, Bacon KM, Bottazzi ME, et al. Global economic burden of Chagas disease: a computational simulation model. *Lancet Infect. Dis.* 2013;13:342-348.
5. Rassi A, Jr., Rassi A, Marin-Neto JA. Chagas disease. *Lancet.* 2010;375:1388-1402.
6. Paucar R, Moreno-Viguri E, Pérez-Silanes S. Challenges in Chagas disease drug discovery: A Review. *Curr. Med. Chem.* 2016;23:3154-3170.
7. WHO. Chagas disease (American trypanosomiasis). http://www.who.int/en/news-room/fact-sheets/detail/chagas-disease-(american-trypanosomiasis); 2018. Accessed 13 March 2019.
8. WHO. Control of Chagas disease: second report of the WHO expert committee. http://www.who.int/iris/handle/10665/42443; 2002. Accessed 14 December 2018.
9. Yamagata Y, Nakagawa J. Control of Chagas disease. *Adv. Parasitol.* 2006;61:129-165.
10. Pérez-Molina JA, Perez AM, Norman FF, et al. Old and new challenges in Chagas disease. *Lancet Infect. Dis.* 2015;15:1347-1356.
11. Dias JC. Evolution of Chagas disease screening programs and control programs: historical perspective. *Glob. Heart.* 2015;10:193-202.
12. Tarleton RL, Gürtler RE, Urbina JA, et al. Chagas disease and the London declaration on neglected tropical diseases. *PLoS Negl. Trop. Dis.* 2014;8:e3219.
13. Clayton J. Chagas disease 101. *Nature.* 2010;465:S4.
14. Oliveira GBF, Avezum Á, Cordeiro Mattos AJ. Perspectives in Chagas disease treatment. *Glob. Heart.* 2015;10:189-192.
15. Bermudez J, Davies C, Simonazzi A, et al. Current drug therapy and pharmaceutical challenges for Chagas disease. *Acta Trop.* 2016;156:1-16.
16. Bern C. Chagas' disease. *N. Engl. J. Med.* 2015;373:456-466.
17. Patterson S, Wyllie S. Nitro drugs for the treatment of trypanosomatid diseases: past, present, and future prospects. *Trends Parasitol.* 2014;30:289-298.
18. Bern C, Montgomery SP, Herwaldt BL, et al. Evaluation and treatment of Chagas disease in the United States: a systematic review. *Jama.* 2007;298:2171-2181.
19. Suryadevara PK, Olepu S, Lockman JW, et al. Structurally simple inhibitors of lanosterol 14α-demethylase are efficacious in a rodent model of acute Chagas disease. *J Med Chem.* 2009;52:3703-3715.

ACCEPTED MANUSCRIPT

20. Keenan M, Abbott MJ, Alexander PW, et al. Analogues of fenarimol are potent inhibitors of Trypanosoma cruzi and are efficacious in a murine model of Chagas disease. *J Med Chem.* 2012;55:4189-4204.
21. Sales Junior PA, Molina I, Fonseca Murta SM, et al. Experimental and clinical treatment of Chagas disease: a review. *Am. J. Trop. Med. Hyg.* 2017;97:1289-1303.
22. Silva DG, Gillespie JR, Ranade RM, et al. New class of antitrypanosomal agents based on imidazopyridines. *ACS Med Chem Lett.* 2017;8:766-770.
23. Bonardi A, Vermelho AB, da Silva Cardoso V, et al. N-nitrosulfonamides as carbonic anhydrase inhibitors: a promising chemotype for targeting Chagas disease and leishmaniasis. *ACS Med. Chem. Lett.* 2018;10:413-418.
24. Hulpia F, Van Hecke K, França da Silva C, et al. Discovery of novel 7-aryl 7-deazapurine 3′-deoxy-ribofuranosyl nucleosides with potent activity against Trypanosoma cruzi. *J Med Chem.* 2018;61:9287-9300.
25. Diniz LdF, Mazzeti AL, Caldas IS, et al. Outcome of E1224-benznidazole combination treatment for infection with a multidrug-resistant Trypanosoma cruzi strain in mice. *Antimicrob. Agents Chemother.* 2018;62:e00401-18.
26. Molina I, Gómez i Prat J, Salvador F, et al. Randomized trial of posaconazole and benznidazole for chronic Chagas' disease. *N. Engl. J. Med.* 2014;370:1899-1908.
27. Morillo CA, Waskin H, Sosa-Estani S, et al. Benznidazole and posaconazole in eliminating parasites in asymptomatic T. cruzi carriers: the STOP-CHAGAS trial. *J. Am. Coll. Cardiol.* 2017;69:939-947.
28. Francisco AF, Lewis MD, Jayawardhana S, et al. Limited ability of posaconazole to cure both acute and chronic Trypanosoma cruzi infections revealed by highly sensitive in vivo imaging. *Antimicrob. Agents Chemother.* 2015;59:4653-4661.
29. Torrico F, Gascon J, Ortiz L, et al. Treatment of adult chronic indeterminate Chagas disease with benznidazole and three E1224 dosing regimens: a proof-of-concept, randomised, placebo-controlled trial. *Lancet Infect Dis.* 2018;18:419-430.
30. Diniz LdF, Urbina JA, de Andrade IM, et al. Benznidazole and posaconazole in experimental Chagas disease: positive interaction in concomitant and sequential treatments. *PLoS Negl Trop Dis.* 2013;7:e2367.
31. Sheng Y, Abreu IA, Cabelli DE, et al. Superoxide dismutases and superoxide reductases. *Chemical Reviews.* 2014;114:3854-3918.
32. Mateo H, Marín C, Pérez-Cordón G, et al. Purification and biochemical characterization of four iron superoxide dismutases in Trypanosoma cruzi. *Mem. Inst. Oswaldo Cruz.* 2008;103:271-276.
33. Villagrán ME, Marín C, Rodriguez-Gonzalez I, et al. Use of an iron superoxide dismutase excreted by Trypanosoma cruzi in the diagnosis of Chagas disease: seroprevalence in rural zones of the state of Queretaro, Mexico. *Am. J. Trop. Med. Hyg.* 2005;73:510-516.
34. Beltran-Hortelano I, Perez-Silanes S, Galiano S. Trypanothione reductase and superoxide dismutase as current drug targets for Trypanosoma cruzi: an overview of compounds with activity against Chagas disease. *Curr. Med. Chem.* 2017;24:1066-1138.
35. Lee B, Bauer H, Melchers J, et al. Irreversible inactivation of Trypanothione reductase by unsaturated Mannich bases: a divinyl ketone as key intermediate. *J. Med. Chem.* 2005;48:7400-7410.
36. Wenzel IN, Wong PE, Maes L, et al. Unsaturated Mannich bases active against multidrug-resistant Trypanosoma brucei brucei strains. *ChemMedChem.* 2009;4:339-351.
37. Roman G. Mannich bases in medicinal chemistry and drug design. *Eur. J. Med. Chem.* 2015;89:743-816.
38. Martin-Montes A, Santivañez-Veliz M, Moreno-Viguri E, et al. In vitro antileishmanial activity and iron superoxide dismutase inhibition of arylamine Mannich base derivatives. *Parasitology.* 2017;144:1783-1790.
39. Davioud-Charvet E, McLeish MJ, Veine DM, et al. Mechanism-based inactivation of thioredoxin reductase from Plasmodium falciparum by Mannich bases. implication for cytotoxicity. *Biochemistry.* 2003;42:13319-13330.

ACCEPTED MANUSCRIPT

ACCEPTED MANUSCRIPT

40. Martín-Escolano R, Moreno-Viguri E, Santiváñez Veliz MJ, et al. Second generation of Mannich base type derivatives with in vivo activity against Trypanosoma cruzi. *J. Med. Chem.* 2018;61:5643-5663.
41. Moreno-Viguri E, Jiménez-Montes C, Martin-Escolano R, et al. In vitro and in vivo anti-Trypanosoma cruzi activity of new arylamine Mannich base-type derivatives. *J. Med. Chem.* 2016;59:10929-10945.
42. Brasil PF, de Freitas JA, Barreto ALS, et al. Antiproliferative and ultrastructural effects of phenethylamine derivatives on promastigotes and amastigotes of Leishmania (Leishmania) infantum chagasi. *Parasitol. Int.* 2017;66:47-55.
43. Damljanović I, Stevanović D, Pejović A, et al. Antibacterial 3-(arylamino)-1-ferrocenylpropan-1-ones: synthesis, spectral, electrochemical and structural characterization. *J. Organomet. Chem.* 2011;696:3703-3713.
44. Bugarin A, Jones KD, Connell BT. Efficient, direct α-methylenation of carbonyls mediated by diisopropylammonium trifluoroacetate. *Chem. Commun.* 2010;46:1715-1717.
45. Gupta SD, Bommaka MK, Mazaira GI, et al. Molecular docking study, synthesis and biological evaluation of Mannich bases as Hsp90 inhibitors. *Int. J. Biol. Macromol.* 2015;80:253-259.
46. Sumita K, Koumori M, Ohno S. A modified Mannich reaction using 1, 3-dioxolane. *Chem. Pharm. Bull.* 1994;42:1676-1678.
47. Zingales B. Trypanosoma cruzi genetic diversity: Something new for something known about Chagas disease manifestations, serodiagnosis and drug sensitivity. *Acta Trop.* 2018;184:38-52.
48. Zingales B, Miles MA, Moraes CB, et al. Drug discovery for Chagas disease should consider Trypanosoma cruzi strain diversity. *Mem. Inst. Oswaldo Cruz.* 2014;109:828-833.
49. Katsuno K, Burrows JN, Duncan K, et al. Hit and lead criteria in drug discovery for infectious diseases of the developing world. *Nat. Rev. Drug Discov.* 2015;14:751.
50. Nwaka S, Ramirez B, Brun R, et al. Advancing Drug Innovation for Neglected Diseases-Criteria for Lead Progression. *PLoS Negl. Trop. Dis.* 2009;3:e440.
51. Romanha AJ, Castro SLd, Soeiro MdNC, et al. In vitro and in vivo experimental models for drug screening and development for Chagas disease. *Mem. Inst. Oswaldo Cruz.* 2010;105:233-238.
52. Scarim CB, Jornada DH, Chelucci RC, et al. Current advances in drug discovery for Chagas disease. *Eur. J. Med. Chem.* 2018;155:824-838.
53. Maldonado CR, Marín C, Olmo F, et al. In vitro and in vivo trypanocidal evaluation of nickel complexes with an azapurine derivative against Trypanosoma cruzi. *J. Med. Chem.* 2010;53:6964-6972.
54. DND*i*. Chagas disease target product profile. https://www.dndi.org/diseases-projects/chagas/chagas-target-product-profile/; 2019. Accessed 13 March 2019.
55. Canavaci AMC, Bustamante JM, Padilla AM, et al. In vitro and in vivo high-throughput assays for the testing of anti-Trypanosoma cruzi compounds. *PLoS Negl. Trop. Dis.* 2010;4:e740.
56. Bustamante JM, Craft JM, Crowe BD, et al. New, combined, and reduced dosing treatment protocols cure Trypanosoma cruzi infection in mice. *J. Infect. Dis.* 2014;209:150-162.
57. Pereira MES, Santos LMT, Araújo MSS, et al. Recrudescence induced by cyclophosphamide of chronic Trypanosoma cruzi infection in mice is influenced by the parasite strain. *Mem. Inst. Oswaldo Cruz.* 1996;91:71-74.
58. Martins HR, Figueiredo LM, Valamiel-Silva JCO, et al. Persistence of PCR-positive tissue in benznidazole-treated mice with negative blood parasitological and serological tests in dual infections with Trypanosoma cruzi stocks from different genotypes. *J. Antimicrob. Chemother.* 2008;61:1319-1327.
59. López-Céspedes Á, Villagrán E, Briceño Álvarez K, et al. Trypanosoma cruzi: seroprevalence detection in suburban population of Santiago de Querétaro (Mexico). *ScientificWorldJournal.* 2012;2012:914129.
60. Olmo F, Gómez-Contreras F, Navarro P, et al. Synthesis and evaluation of in vitro and in vivo trypanocidal properties of a new imidazole-containing nitrophthalazine derivative. *Eur. J. Med. Chem.* 2015;106:106-119.
61. Kayama H, Takeda K. The innate immune response to Trypanosoma cruzi infection. *Microbes Infect.* 2010;12:511-517.

ACCEPTED MANUSCRIPT

62. Francisco AF, Jayawardhana S, Lewis MD, et al. Nitroheterocyclic drugs cure experimental Trypanosoma cruzi infections more effectively in the chronic stage than in the acute stage. *Sci Rep.* 2016;6:35351.
63. Ginger ML. Trypanosomatid biology and euglenozoan evolution: new insights and shifting paradigms revealed through genome sequencing. *Protist.* 2005;156:377-392.
64. Maugeri DA, Cannata JJB, Cazzulo JJ. Glucose metabolism in Trypanosoma cruzi. *Essays Biochem.* 2011;51:15-30.
65. Cazzulo JJ. Aerobic fermentation of glucose by trypanosomatids. *FASEB J.* 1992;6:3153-3161.
66. Bringaud F, Rivière L, Coustou V. Energy metabolism of trypanosomatids: Adaptation to available carbon sources. *Mol. Biochem. Parasitol.* 2006;149:1-9.
67. Kirkinezos IG, Moraes CT. Reactive oxygen species and mitochondrial diseases. *Semin. Cell Dev. Biol.* 2001;12:449-457.
68. Lee WK, Thévenod F. A role for mitochondrial aquaporins in cellular life-and-death decisions? *Am. J. Physiol., Cell Physiol.* 2006;291:C195-C202.
69. Shang XJ, Yao G, Ge JP, et al. Procyanidin induces apoptosis and necrosis of prostate cancer cell line PC-3 in a mitochondrion-dependent manner. *J. Androl.* 2009;30:122-126.
70. Hall BS, Wilkinson SR. Activation of benznidazole by trypanosomal type I nitroreductases results in glyoxal formation. *Antimicrob. Agents Chemother.* 2012;56:115-123.
71. McDaniels AE, Reyes AL, Wymer LJ, et al. Comparison of the Salmonella (Ames) test, Umu tests, and the sos chromotests for detecting genotoxins. *Environ. Mol. Mutagen.* 1990;16:204-215.
72. OECD, Test No. 471: Bacterial reverse mutation test, 1997.
73. Ferreira R, Ferreira L. Mutagenicity of nifurtimox and benznidazole in the Salmonella/microsome assay. *Braz. J. Med. Biol. Res.* 1986;19:19-25.
74. Melo MEB, Ferreira LCS. Screening the mutagenic activities of coomonly used antiparasite drugs by the Simultest, a simplified Salmonella/microsome plate incorporation assay. *Rev. Inst. Med. Trop. Sao Paulo.* 1990;32:269-274.
75. Hanaki E, Hayashi M, Matsumoto M. Delamanid is not metabolized by Salmonella or human nitroreductases: A possible mechanism for the lack of mutagenicity. *Regul. Toxicol. Pharmacol.* 2017;84:1-8.
76. Martinez A, Peluffo G, Petruk AA, et al. Structural and molecular basis of the peroxynitrite-mediated nitration and inactivation of Trypanosoma cruzi Fe-superoxide dismutases A and B: disparate susceptibilities due to the repair of Tyr35 radical by Cys83 in Fe-SODB through intramolecular electron transfer. *J. Biol. Chem.* 2014;289:12760-12778.
77. Pettersen EF, Goddard TD, Huang CC, et al. UCSF Chimera—a visualization system for exploratory research and analysis. *J. Comput. Chem.* 2004;25:1605-1612.
78. Fulmer GR, Miller AJM, Sherden NH, et al. NMR chemical shifts of trace impurities: common laboratory solvents, organics, and gases in deuterated solvents relevant to the organometallic chemist. *Organometallics.* 2010;29:2176-2179.
79. Garnica P, Encío I, Plano D, et al. Combined acylselenourea–diselenide structures: new potent and selective antitumoral agents as autophagy activators. *ACS Med. Chem. Lett.* 2018;9:306-311.
80. Téllez-Meneses J, Mejía-Jaramillo AM, Triana-Chávez O. Biological characterization of Trypanosoma cruzi stocks from domestic and sylvatic vectors in Sierra Nevada of Santa Marta, Colombia. *Acta Trop.* 2008;108:26-34.
81. Olmo F, Marín C, Clares MP, et al. Scorpiand-like azamacrocycles prevent the chronic establishment of Trypanosoma cruzi in a murine model. *Eur. J. Med. Chem.* 2013;70:189-198.
82. Rampersad SN. Multiple applications of alamar blue as an indicator of metabolic function and cellular health in cell viability bioassays. *Sensors.* 2012;12:12347–12360.
83. Cardoso J, Soares MJ. In vitro effects of citral on Trypanosoma cruzi metacyclogenesis. *Mem. Inst. Oswaldo Cruz.* 2010;105:1026-1032.
84. Olmo F, Cussó O, Marín C, et al. In vitro and in vivo identification of tetradentated polyamine complexes as highly efficient metallodrugs against Trypanosoma cruzi. *Exp. Parasitol.* 2016;164:20-30.

ACCEPTED MANUSCRIPT

ACCEPTED MANUSCRIPT

85. Martín-Escolano R, Aguilera-Venegas B, Marín C, et al. Synthesis and Biological in vitro and in vivo Evaluation of 2-(5-Nitroindazol-1-yl)ethylamines and Related Compounds as Potential Therapeutic Alternatives for Chagas Disease. *ChemMedChem.* 2018;13:2104-2118.
86. Olmo F, Clares MP, Marín C, et al. Synthetic single and double aza-scorpiand macrocycles acting as inhibitors of the antioxidant enzymes iron superoxide dismutase and trypanothione reductase in Trypanosoma cruzi with promising results in a murine model. *RSC Adv.* 2014;4:65108-65120.
87. Pérez-Silanes S, Torres E, Arbillaga L, et al. Synthesis and biological evaluation of quinoxaline di-N-oxide derivatives with in vitro trypanocidal activity. *Bioorg. Med. Chem. Lett.* 2016;26:903-906.
88. Olmo F, Guardia JJ, Marin C, et al. Prospects of an alternative treatment against Trypanosoma cruzi based on abietic acid derivatives show promising results in Balb/c mouse model. *Eur. J. Med. Chem.* 2015;89:683-690.
89. Olmo F, Rotger C, Ramírez-Macías I, et al. Synthesis and biological evaluation of N,N′-squaramides with high in vivo efficacy and low toxicity: toward a low-cost drug against Chagas disease. *J. Med. Chem.* 2014;57:987-999.
90. Caballero AB, Marín C, Rodríguez-Diéguez A, et al. In vitro and in vivo antiparasital activity against Trypanosoma cruzi of three novel 5-methyl-1,2,4-triazolo[1,5-a]pyrimidin-7(4H)-one-based complexes. *J. Inorg. Biochem.* . 2011;105:770-776.
91. Fernández- Becerra C, Sánchez- Moreno M, Osuna A, et al. Comparative aspects of energy metabolism in plant trypanosomatids. *J. Eukaryot. Microbiol.* 1997;44:523-529.
92. Sandes JM, Fontes A, Regis-da-Silva CG, et al. Trypanosoma cruzi cell death induced by the Morita-Baylis-Hillman adduct 3-hydroxy-2-methylene-3-(4-nitrophenylpropanenitrile). *PLoS One.* 2014;9:e93936.
93. Bradford MM. A rapid and sensitive method for the quantitation of microgram quantities of protein utilizing the principle of protein-dye binding. *Anal. Biochem.* 1976;72:248-254.
94. Beyer Jr WF, Fridovich I. Assaying for superoxide dismutase activity: some large consequences of minor changes in conditions. *Anal. Biochem.* 1987;161:559-566.
95. Hanwell MD, Curtis DE, Lonie DC, et al. Avogadro: an advanced semantic chemical editor, visualization, and analysis platform. *J. Cheminformatics.* 2012;4:17.
96. Martinez A, Peluffo G, Petruk AA, et al. Structural and Molecular Basis of the Peroxynitrite-mediated Nitration and Inactivation of Trypanosoma cruzi Iron-Superoxide Dismutases (Fe-SODs) A and B: Disparate Susceptibilities due to the repair of TYR(35) radical by CYS(83) in Fe-SODB through intramolecular electron transfer. *J. Biol. Chem.* 2014;289:12760-12778.
97. Dolinsky TJ, Czodrowski P, Li H, et al. PDB2PQR: expanding and upgrading automated preparation of biomolecular structures for molecular simulations. *Nucleic Acids Res.* 2007;35:W522-W525.
98. Morris GM, Huey R, Lindstrom W, et al. AutoDock4 and AutoDockTools4: automated docking with selective receptor flexibility. *J Comput Chem.* 2009;30:2785-2791.
99. Huey R, Morris GM, Olson AJ, et al. A semiempirical free energy force field with charge- based desolvation. *J Comput Chem.* 2007;28:1145-1152.

ACCEPTED MANUSCRIPT

ACCEPTED MANUSCRIPT

- Novel Mannich bases have been designed, synthesized and characterised.
- Compounds **7** and **9** presented the best *in vitro* efficacy and safety profile.
- Compound **9** exhibited an encouraging *in vivo* efficacy against *T. cruzi*.
- The mechanism of action proposed the inhibition of iron superoxide dismutase.

ACCEPTED MANUSCRIPT